



**HAL**  
open science

## Non-classical ligand-independent regulation of Go protein by an orphan Class C GPCR

Mariana Hajj, Teresa de Vita, Claire Vol, Charlotte Renassia, Jean-Charles Bologna, Isabelle Brabet, Magali Cazade, Manuela Pastore, Jaroslav Blahos, Gilles Labesse, et al.

### ► To cite this version:

Mariana Hajj, Teresa de Vita, Claire Vol, Charlotte Renassia, Jean-Charles Bologna, et al.. Non-classical ligand-independent regulation of Go protein by an orphan Class C GPCR. *Molecular Pharmacology*, 2019, 96 (2), pp.233-246. 10.1124/mol.118.113019 . hal-02396282

**HAL Id: hal-02396282**

**<https://hal.science/hal-02396282v1>**

Submitted on 5 Dec 2019

**HAL** is a multi-disciplinary open access archive for the deposit and dissemination of scientific research documents, whether they are published or not. The documents may come from teaching and research institutions in France or abroad, or from public or private research centers.

L'archive ouverte pluridisciplinaire **HAL**, est destinée au dépôt et à la diffusion de documents scientifiques de niveau recherche, publiés ou non, émanant des établissements d'enseignement et de recherche français ou étrangers, des laboratoires publics ou privés.

# **Non-classical ligand-independent regulation of Go protein by an orphan Class C GPCR**

Mariana Hajj, Teresa De Vita, Claire Vol, Charlotte Renassia, Jean-Charles Bologna, Isabelle Brabet, Magali Cazade, Manuela Pastore, Jaroslav Blahos, Gilles Labesse, Jean-Philippe Pin, Laurent Prézeau

IGF, Univ. Montpellier, CNRS, INSERM, Montpellier, France: MH, TDV, CV, CR, JCB, IB, MC, MP, JPP, LP

Institute of Molecular Genetics, Academy of Sciences of the Czech Republic and Department of Pharmacology, 2nd Medical School, Charles University, Prague, Czech Republic: JB

CBS, Univ. Montpellier, CNRS, INSERM, Montpellier, France: GL

**Running title:** Atypical ligand-independent control of Go by GPR158

**Corresponding author:**

Laurent Prézeau

IGF, 141, rue de la Cardonille, 34094 Montpellier, cedex 05

Tel.: +33(0) 434 35 92 96 - Fax.: +33(0) 467 54 24 42 - Email: [Laurent.prezeau@igf.cnrs.fr](mailto:Laurent.prezeau@igf.cnrs.fr)

- 28 pages of text and 6 pages of Legends

- 0 Tables

- 8 Figures (and 6 Supplemental DATA)

- 50 References

- Abstract: 244 words

- Introduction: 744 words

- Discussion: 1899 words

**List of nonstandard abbreviations**

AGS: Activator of G protein Signaling

BRET: Bioluminescence Resonance Energy Transfer

CRD: Cysteine-Rich Domain

ECD: Extracellular Domain

GEF: G protein nucleotide Exchange Factor

HTRF®: Homogenous Time-Resolved FRET

LRET: Luminescence Resonance Energy Transfer

RGS: Regulatory of G protein Signaling

TR-FRET: Time-Resolved Förster Resonance energy transfer

**Abstract**

The orphan G protein-coupled receptor (GPCR) GPR158 is expressed in the brain, where it is involved in the osteocalcin effect on cognitive processes, and at the periphery where it may contribute to glaucoma and cancers. GPR158 forms a complex with RGS7- $\beta$ 5 leading to the regulation of neighboring GPCR-induced Go protein activity. Intriguingly, GPR158 also interacts with  $\alpha$ o although no canonical Go coupling has been reported. GPR158 displays three VCPWE motifs in its C-terminal domain putatively involved in G protein regulation. Here, we addressed the scaffolding function of GPR158 and its VCPWE motifs on Go. We observed that GPR158 interacted with and stabilized the amount of RGS7- $\beta$ 5 through a 50-residue region downstream of its transmembrane domain and upstream of the VCPWE motifs. We show that two VCPWE motifs are involved in  $\alpha$ o binding. Using a  $G\alpha$ o- $\beta$  $\gamma$  BRET sensor we found that GPR158 decreases the BRET signal as observed upon G protein activation. However, no constitutive activity of GPR158 could be detected through the measurement of various G protein-mediated downstream responses. We propose that the effect of GPR158 on Go is unlikely due to a canonical activation of Go, but rather to the trapping of  $G\alpha$ o by the VCPWE motifs possibly leading to its dissociation from  $\beta$  $\gamma$ . Such action of GPR158 is expected to prolong the  $\beta$  $\gamma$  activity as also observed with some Activators of G protein Signaling (AGS). Taken together our data revealed a complex functional scaffolding/signaling role for GPR158 controlling Go through an original mechanism.



## **Introduction**

G protein-coupled receptors (GPCRs) are key players in cell-cell communication and the protein family the most targeted by commercial drugs (Overington et al., 2006). GPCRs couple to heterotrimeric ( $\alpha\beta\gamma$  subunits) G proteins that control the activity of membrane and intracellular effectors. GPCRs behave as G protein nucleotide Exchanging Factors (GEF) to promote the GTP-bound G protein  $\alpha$  subunit active state, generally considered dissociated from  $\beta\gamma$ . Furthermore, G protein  $\alpha$  and  $\beta\gamma$  activities can be decreased by other signaling proteins like Regulators of G Protein Signaling (RGS) (Gerber et al., 2016), or prolonged by Activators of G protein Signaling (AGS) (Blumer and Lanier, 2014). GPCRs have also been shown to mediate their action through G protein-independent pathways (such as those involving arrestins), signaling cross-talk (Prezeau et al., 2010), receptor transactivation (Milligan, 2006), or association with specific signalosomes (Bockaert et al., 2010). Thus, GPCR signaling pathways have to be functionally organized to integrate so many regulatory inputs.

Cellular and physiological functions of the orphan receptor GPR158 are largely unknown. It is expressed in the brain (Orlandi et al., 2015) where it likely regulates neuron excitability as it has been fished out as a partner of potassium Kv4.2 and calcium Cav2 channels (Marionneau et al., 2009; Muller et al., 2010). In the CA3 region of the hippocampus, GPR158 has recently been reported to be involved in the cognitive actions of osteocalcin (Khrimian et al., 2017) and to control the presynaptic differentiation of mossy fiber-CA3 synapses by interacting with proteoglycans of the extracellular matrix (Condomitti et al., 2018). GPR158 could also be involved in the shaping of retinal photoreceptor signaling (Orlandi et al., 2012). Interestingly, its expression is regulated by glucocorticoids in trabecular meshwork cells, a mechanism possibly involved in occurrence of glaucoma (Patel et al., 2013). While its role in prostate cancer emerged recently (Patel et al., 2015), impact of GPR158 mutations in colorectal cancers and leukemia still have to be confirmed (Greif et al., 2011; Wood et al., 2007). Altogether, these data suggest important regulatory roles in cellular processes, highlighting the real necessity in understanding GPR158 signaling roles in healthy and disease cells.

Potential signaling functions for GPR158 is supported by the observation that GPR158 can interact with the RGS7 protein and the G protein  $\alpha_o$  subunit (Orlandi et al., 2012, 2015). Indeed, GPR158 brings RGS7 to the plasma membrane where RGS7 can allosterically accelerate the GTPase

activity of  $G\alpha_o$  and turn it off when  $G_o$  is activated by neighboring GPCRs. Three short VCPWE motifs are present in the last third of the C-terminal domain (C-terminal domain) of GPR158. Although they resemble the ICPWE motif of retinal PDE  $\gamma$  subunit known to mediate the interaction with R7 family RGS proteins and active G protein  $\alpha$  subunits (Slep et al., 2001), they were not involved in RGS7 interaction with GPR158 (Orlandi et al., 2015). Thus, while RGS7 would interact in the first third of the C-terminal domain of GPR158,  $G\alpha_o$  may bind on two sites, one in the same region than RGS7, and another one in the second half of the C-terminal domain. Surprisingly, the role of the VCPWE motifs remains unclear. Furthermore, GPR158 possesses residues signatures reported to be important for G protein coupling of other GPCRs (Bjarnadóttir et al., 2005), but the ability of GPR158 to couple to G proteins in a canonical way has not been addressed either. Thus, it seems that GPR158 plays important roles in the absence of ligand, notably through its association with RGS7. The question remains what the scaffolding role of GPR158 toward RGS7 and  $G_o$  could be in the absence of ligand.

Here we identified the interaction site of RGS7 in the 714-764 region of GPR158 C-terminal domain and confirmed the three VCPWE motifs are not involved in this interaction. In contrast, these motifs were required for  $G\alpha_o$  association. We also show that GPR158 likely induced  $G\alpha_o$ - $\beta\gamma$  dissociation as measured by a BRET assay, reflecting possible activation by the receptor. However, we found no evidence of canonical coupling of WT and GPR158 mutants to G protein under basal condition using second messenger functional assays. Indeed, this GPR158-induced increased levels of dissociated  $G_o$  is possibly due to trapping of  $G\alpha_o$  by the GPR158 VCPWE motifs. By trapping  $G\alpha_o$ , GPR158 is expected to prolong the action of  $\beta\gamma$ , as observed with some group-II AGS proteins. These data, that do not exclude the possible direct G protein activation upon ligand activation of GPR158, unravel new ways for GPCRs to locally regulate G protein pathways.

## **Material & Methods**

### ***Compounds***

All compounds and reagents were purchased from the most appropriate sources and companies.

### ***Plasmids and site-directed mutagenesis***

To generate C-terminal Flag- or HA-tagged GPR158 constructs, HA or Flag tag sequences were introduced downstream of GPR158 coding region after a unique MluI restriction site, followed by a stop codon. To generate the C-terminal truncated forms ( $\Delta$ C1 to  $\Delta$ C11) of GPR158 receptor, a second MluI site was inserted at the required positions and the DNA sequence between the two MluI sites was excised. To generate N-terminal tagged Ha- and Flag-GPR158 constructs, MluI and XbaI restriction sites were inserted by PCR after the N-terminal peptide signal and after the C-terminal stop codon of the GPR158 coding sequence, respectively. The resulted MluI-XbaI fragment was then inserted into pRK-HA- and pRK-Flag-GABA<sub>B1</sub> (GB1) plasmids (Kniazeff et al., 2004; Rives et al., 2009) digested using the MluI and XbaI sites, which excised the GABA<sub>B1</sub> coding sequence. We generated HA-Snap-GPR158 and Flag-Clip-GPR158 by inserting the sequence encoding Snap tag and Clip tag at MluI site of HA-GPR158 and Flag-GPR158, respectively, using a Quick-Change® strategy (Stratagene, San Diego, CA, USA). The RGS7 (s2 form) and  $\beta$ 5 plasmids were purchased from (UMR cDNA Resource center, MO, USA). The HA tag was introduced at the C-terminal end of the coding sequence of RGS7 upstream of both a XhoI restriction site and a stop codon using a Quick-Change® strategy. To generate GABA<sub>B1a</sub>-HA, the HA tag sequence was inserted at the C-terminal end of the GABA<sub>B1a</sub> coding sequence between a XhoI site and the stop codon using a Quick-Change® strategy. Chimeras formed by exchanging domain between mGlu1a and GPR158 or mGlu2 and GPR158 were generated using PCR overlap strategies and point mutations in GPR158 sequence were generated using the Quick-Change® strategy. All final constructs were verified by sequencing (MWG, Ebersberg, Germany).

### ***Cell culture and transfection***

HEK-293 cells (from ATCC) were cultured in Dulbecco's modified Eagle's medium (DMEM, Invitrogen Life Technologies, Gaithersburg, MD), supplemented with 10 % fetal calf serum (SIGMA, L'isle-D'Abeau, Saint-Quentin Fallavier, France), cultures were checked each month

for mycoplasma. The cells were seeded out in 100 mm plates and incubated at 37°C in a CO<sub>2</sub> incubator. Cells were transiently transfected using Lipofectamine 2000 following the manufacturer's protocol (Thermo Fisher Scientific, Waltham, MS, USA). Cells were seeded in 96 well plates (Greiner bio-One, Frickenhausen, Germany) at 50,000 or 100,000 cells per well. Alternatively, cells were transfected by electroporation as previously described (Maurel et al., 2004). Ten million cells were electroporated with indicated plasmids containing the coding sequence of the proteins of interest and completed to a total amount of 10 µg plasmid DNA with pRK6 empty vector, before plated in 96 well plates. All media used for cell culture were purchased from Life Technologies/Thermo Fisher Scientific (Waltham, MS, USA).

#### ***Extracellular and Intracellular antibody TR-FRET assay (HTRF®)***

Based on a Luminescence Resonance Energy Transfer (LRET) technology, Time-Resolved Förster Resonance Energy Transfer (TR-FRET) experiments using labeled antibodies were performed in 96 well plates in homogenous conditions (HTRF®), as previously described (Maurel et al., 2008). Twenty-four hours after transfection, cells were washed with cold Tris-KREBS buffer (20mM Tris pH 7.4, 118 mM NaCl, 5.6 mM glucose, 1.2 mM KH<sub>2</sub>PO<sub>4</sub>, 1.2 mM MgSO<sub>4</sub>, 4.7 mM KCl, and 1.8 mM CaCl<sub>2</sub>) and incubated overnight at 4°C with lumiphore-conjugated antibodies (Europium Cryptate-labeled antibody (3 nM) and d2- labeled antibody (6 nM)) (Cisbio Bioassays, Codolet, France). The cells were then incubated for 5 min at room temperature with KF (200mM). The fluorescence of the europium cryptate (620 nm) and d2 (665 nm) was measured 50 µs after excitation at 337 nm, using RubyStar or PHERAStar plate readers (BMG Labtechnologies, Champigny-sur-Marne, France). The TR-FRET signals were expressed as  $\% \Delta F = \frac{(665/620)_{\text{sample}} - (665/620)_{\text{mock}}}{(665/620)_{\text{mock}}} * 100$ . For intracellular antibody TR-FRET assay, measurements were performed in cells permeabilized with Triton X-100 0.02% (v/v) prior to overnight incubation at 4°C with lumiphore-conjugated antibodies (Europium Cryptate-labeled antibody (3 nM) and d2- labeled antibody (6 nM)) (Cisbio Bioassays, Codolet, France).

#### ***Cell surface protein level quantification by ELISA and SNAP labeling***

ELISA experiments were performed as previously described (Maurel et al., 2008). Briefly, cells were fixed with 4% paraformaldehyde and blocked with phosphate-buffered saline (PBS) containing 1% fetal calf serum, and then incubated 30 min at 0.5 mg/L with monoclonal anti-Flag M2 antibodies (SIGMA, L'isle-D'Abeau, Saint-Quentin Fallavier, France), anti-HA antibodies

(clone 3F10, Roche Applied Science, Basel, Switzerland), or anti-Myc antibodies (clone 9E10, University of Iowa, Iowa City, IA, USA). When these primary antibodies were not conjugated themselves with horseradish peroxidase (HRP), cells were further washed and incubated (30 min) with HRP-conjugated goat anti-rat IgG (0.5 mg/L, Jackson ImmunoResearch laboratories, Westgrove, PA, USA) or anti-rabbit IgG or anti-mouse IgG (0.5 mg/l, Amersham Biosciences GE Healthcare, Chicago, IL, USA) for 30 min. After washes, bound antibody was detected by chemiluminescence using SuperSignal substrate (Pierce, Rockford, IL, USA) and a Mithras LB 940 plate reader (Berthold Biotechnologies, Bad Wildbad, Germany). As a control for intracellular ELISA quantification, cells were permeabilized for 5 min with 0.05% Triton X-100 just after being fixed. SNAP-tag labeling was performed as described previously (Doumazane et al., 2011). Briefly, 24 h after transfection, HEK293 cells were incubated at 37°C for 1 h with a solution of 100 nM of Lumi4-Tb (Cisbio Bioassays, Codolet, France). After labeling, cells were washed three times with Krebs buffer, and drugs were added as described. TR-FRET measurements were performed on INFINITE 500 (TECAN, Männedorf, SW) or PHERAstar FS (BMG Labtechnologies, Champigny-sur-Marne, France) microplate readers which are equipped a standard with 'TR-FRET' optical modules.

### ***Co-immunoprecipitation and western blotting***

At 48 h after transfection in 100 mm plates, cells were washed with ice-cold PBS-GAB (PBS supplemented with Glucose and Antibiotics). After washes, cells were scraped with PBS-GAB and centrifuged 5 min at 2000 rpm. The supernatant was removed and the pellet was resuspended in Lysis Buffer (Hepes 1M, NaCl 5M, NP40 20%, Glycerol, DDM (dodecyl maltoside), and protease inhibitors cocktail (SIGMA, L'isle-D'Abeau, Saint-Quentin Fallavier, France)). The lysate was incubated for 2 hours at 4°C with mild shaking, and then clarified by centrifugation at 15000 g for 15 min. Clarified lysate was incubated with monoclonal anti-HA conjugate agarose beads, (Clone HA-7, SIGMA, L'isle-D'Abeau, Saint-Quentin Fallavier, France) overnight at 4°C then centrifuged for 2 min at 13000 rpm. The supernatant was removed and the pelleted beads were washed four times with PBS 1X before elution by addition of loading buffer. The samples were loaded on NuPAGE® Novex 3-8% Tris-Acetate Midi Gel (Invitrogen Life Technologies, Gaithersburg, MD, USA) transferred to nitrocellulose membrane (Amersham Biosciences GE Healthcare, Chicago, IL, USA) and subjected to immunoblotting. The primary rabbit anti-HA

(Invitrogen Life Technologies, Gaithersburg, MD, USA) antibody was used at 0.6 mg/L and the mouse anti-Flag antibody (Sigma, F3165) at 2mg/L. Secondary antibodies anti-rabbit HRP-linked IgG (0.5 mg/L, Amersham Biosciences GE Healthcare, Chicago, IL, USA) and anti-mouse HRP-linked IgG (Santa Cruz, Dallas, TX, USA) were applied for 30min. Immunoreactive bands were visualized by ECL detection kit (Amersham Biosciences GE Healthcare, Chicago, IL, USA) on Kodak ML light films.

### ***IP-one and cAMP assays***

Experiments were performed in a 96 well plate format. The IPOne HTRF® kit (Cisbio Bioassays, Codolet, France) was used according to the recommendations of the manufacturer to measure the production of inositol phosphate second messengers (IP<sub>3</sub>), through assessment of IP<sub>1</sub> accumulation, a downstream metabolite of IP<sub>3</sub>. Cells were incubated in presence of indicated receptor agonist for 30 min at 37°C and then incubated in presence of a cryptate-labelled anti-IP<sub>1</sub> or cAMP antibodies and D<sub>2</sub>-labeled IP<sub>1</sub> or cAMP for 1 hour at room temperature. The fluorescence of the europium cryptate and d<sub>2</sub>, 620 nm and 665 nm respectively, was measured (without washing) 50 μs after excitation at 337 nm using RubyStar or PHERAstar plate readers (BMG Labtechnologies, Champigny-sur-Marne, France).

### ***BRET experiments***

As previously described (Ayoub et al., 2007) for saturation curves, a constant amount of a plasmid encoding one of the proteins of interest bearing the donor-Luc was co-expressed with a range of expression of the plasmid encoding the second protein of interest bearing the acceptor-YFP. After washing of the cells, the Luciferase substrate Coelenterazine h (Cat. No. C-6780 Invitrogen/ Thermo Fisher Scientific, Waltham, MS, USA,) was added (5 mM in 50 μl per well) to initiate the BRET process. Readings were recorded using the Mithras LB940 reader (Berthold Biotechnologies, Bad Wildbad, Germany) (Rluc filter: 485±20 nm and YFP filter: 530±25 nm), data was collected using the MicroWin2000 software, and BRET signal expressed in milliBRET units of BRET ratio. Dose-response curves were fitted with a linear regression or sigmoid dose-response equation, using Prism (GraphPad software, San Diego, USA). The Gα<sub>o</sub> experiments were performed as previously described (Rives et al., 2009). The Go activation/dissociation BRET assays was performed as described previously (Brulé et al., 2014). The transfected HEK293 cells were washed with PBS, and readout was performed on a Mithras LB940 plate reader (Berthold

Technologies, Bad Wildbad, Germany) at 37°C after the addition of coelenterazine h (5 µM) and ligand. When indicated, treatment with Pertussis Toxin (100 ng/mL) was performed for 16h before stimulation of the cells. The BRET ratio was calculated on the basis of the difference of the emission at 530 nm/485 nm of co-transfected Rluc and YFP fusion proteins and the emission at 530 nm/485 nm of the Rluc fusion protein alone.

***Data analysis and statistical tests***

Data were analyzed using Prism 7.0e (GraphPad) or Excel 16.16.8 (Microsoft), and statistical tests were performed using Prism tutorial and R software.

## **Results**

### **GPR158 forms homodimers at the cell surface**

The orphan receptor GPR158 shares homology within its 7 transmembrane (7TM) domain with the class C GPCRs (Bjarnadóttir et al., 2005), including the metabotropic glutamate (mGlu) and GABA (GABA<sub>B</sub>) receptors. Like most class C GPCRs, GPR158 also has a large N-terminal extracellular domain linked to the 7TM domain via a cysteine-rich domain (CRD). However, neither parts of the N-terminal domain are related to those of the class C GPCRs (Kniazeff et al., 2011). The N-terminal part of most class C GPCRs, called the Venus flytrap (VFT) domain contains the agonist binding site and is responsible for the constitutive dimerization of these receptors (Koehl et al., 2019; Pin and Bettler, 2016).

We observed that like most Class C GPCRs, GPR158 also exists as homodimers at the surface of transfected HEK293 cells. Indeed, western blots showed two major bands possibly corresponding to GPR158 monomers and dimers, regardless which antibodies were used to reveal the protein (Fig.1A). Moreover, N-terminally HA epitope-tagged GPR158 (HA-GPR158) co-immunoprecipitated N-terminally Flag epitope-tagged GPR158 (Flag-GPR158) co-expressed in HEK293 cells (Fig.1B). In contrast, neither Flag-mGlu2 nor the Flag-GB2 subunit of the GABA<sub>B</sub> receptor co-immunoprecipitated with HA-GPR158 receptor (Fig.1B), while HA-GB2 association to its Flag-GB1 subunit partner could easily be detected (Fig.1B). Cellular dimeric TR-FRET signals (Maurel et al., 2008) were detected using anti-HA and anti-Flag antibodies labeled with LRET-compatible dyes in cells co-expressing HA-GPR158 and Flag-GPR158, but not in cells co-expressing Flag-GPR158 and HA-GB2 (Fig.1C, D). Finally, Flag-GPR158 homodimer formation was disrupted by increasing amount of HA-GPR158 but not by HA-GB2 (Fig.1E). Taken together, these data indicate that GPR158, like the other class C GPCRs forms homodimers at the cell surface. Given this stoichiometry is a mandatory feature of functional class C GPCRs (El Moustaine et al., 2012), this pushed us to analyze any possible functional role of GPR158. We first further explored the role of its intracellular domain already reported to interact with G protein mediating signaling proteins, including Go and RGS7.

### **RGS7 protein level is stabilized by a specific region of GPR158 C-terminal domain**



In transiently transfected HEK293 cells, GPR158, but not the related GB2 GABA<sub>B</sub> subunit, interacted with RGS7 and not with RGS4, as shown by co-immunoprecipitation (Fig.2A, B). In these experiments the G protein subunit  $\beta 5$  was co-expressed with RGS7 as it forms a stable complex with RGS7 and protects it from proteolytic degradation (Anderson et al., 2009) (Supplemental Figure 1A). The RGS7: $\beta 5$  interaction with GPR158 was confirmed by a TR-FRET approach (Supplemental Figure 1B). Indeed, a large TR-FRET signal was measured in cells expressing C-terminally Flag-tagged GPR158 (GPR158-Flag) and RGS7-HA, incubated with TR-FRET compatible anti-HA or anti-Flag antibodies, following cell permeabilization. Interestingly, no signal was observed between GPR158 and RGS4-HA. The differential signal measured between RGS7-HA and RGS4-HA expressing cells was not due to different levels of these two proteins nor to a differential amount of GPR158 (Fig.2A, Supplemental Figure 1B).

Using membrane targeting microscopy and *in vitro* co-immunoprecipitation assays, Orlandi *et al.* reported that RGS7 interacted with the C-terminal domain of GPR158 (Orlandi et al., 2015). In agreement with this observation, we found that the C-terminal truncated forms of GPR158, which ended at residues Ser692 (GPR158- $\Delta$ C1) or Ser699 (GPR158- $\Delta$ C2) (Fig.2C), did not co-immunoprecipitate RGS7 (Fig.2D, E). No significant intracellular TR-FRET signal with RGS7 could also be measured with these cropped GPR158 mutants (Fig.2F), despite protein levels similar to that of WT (Fig.2D-F). Unexpectedly, the three conserved VCPWE motifs of GPR158 (Fig.3A, Supplemental Figure 2) were not involved in RGS7 binding (Fig.3B, C), despite their similarity to the PDE  $\gamma$ -subunit motif known to participate in complex formation with the RGS7-related RGS9 protein (Slep et al., 2001). Indeed, the mutation of the three motifs individually (GPR158-Mut1, -Mut2, and -Mut3) or in combination (GPR158-Mut4) (Fig.3A), did not suppress GPR158:RGS7 interaction measured either by co-immunoprecipitation (Fig.3B) or TR-FRET (Fig.3C) approaches.

Using a series of GPR158-Flag C-terminal deletion mutants (GPR158- $\Delta$ C1 to - $\Delta$ C11, Fig.3D), we identified the region encompassing residues 714 to 764 as the RGS7 binding site using both co-immunoprecipitation and TR-FRET approaches (Fig.3E, F). The 714-764 region overlaps with the region reported by Orlandi *et al.* to contribute to RGS7 binding (Orlandi et al., 2015). We found that this GPR158:RGS7 interaction enhanced RGS7 abundance either in absence or presence of its  $\beta 5$  partner (Fig.4 and Supplemental Figure 3). Using a constant amount of

transfected RGS7-coding plasmid, RGS7 protein level was increased in HEK293 cells co-expressing increasing levels of GPR158 (Fig.4A, B), but not in cells expressing either mGlu2 (Fig.4A) or GPR158- $\Delta$ C1 (Fig.4B). Of note, expression of mGlu2 actually led to decreased level of RGS7 protein (Fig.4A). Whether this is due to mGlu2 itself, or to its constant activity due to ambient glutamate in cell culture media remains to be clarified. The enhancing effect exerted by GPR158 was less pronounced in the absence of  $\beta$ 5 (Supplemental Figure 3). Such a stabilizing effect involves the RGS7 binding domain of GPR158 as revealed using a series of mGlu2 chimeric constructs containing the WT or mutated C-terminal domain of GPR158 (Supplemental Figure 4A&B).

These data identified a specific region in the C terminal domain of GPR158, not including the VCPWE motifs, interacting with and stabilizing RGS7: $\beta$ 5. We then wondered whether these VCPWE motifs were involved in the interaction with  $G\alpha_o$ , a RGS7-regulated G protein subunit that has been reported to interact with the C-terminal domain of GPR158 (Orlandi et al., 2012, 2015).

### **VCPWE motifs contribute to $G\alpha_o$ binding**

We first confirmed the interaction between GPR158 and  $G\alpha_o$  using both TR-FRET (Fig.5A) and BRET approaches (Fig.5B). Indeed, the GPR158 and  $G\alpha_o$  interaction was supported by the generation of a saturating BRET signal curve (Fig.5B) in HEK293 cells expressing various expression ratios of GPR158-Venus and  $G\alpha_o$ -RLuc. In contrast, a non-specific, linear low BRET signal curve was obtained in control cells expressing GPR158-Venus and Homer3-RLuc (Fig.5B), an mGlu receptor interacting intracellular protein (Rives et al., 2009). Interestingly, a saturating BRET curve was also observed in cells expressing GPR158-Venus and the  $G\alpha_o$ -related  $G\alpha_i$ -RLuc protein, while no BRET signal could be detected with  $G\alpha_q$ -RLuc (Fig.5C), suggesting GPR158 can interact with the  $G\alpha_i/o$  protein family members but not with  $G\alpha_q$ . We then showed that the C-terminal domain of GPR158 was required for this interaction, since the TR-FRET signal was greatly reduced in cells expressing  $G\alpha_o$ -Flag and the truncated GPR158- $\Delta$ C1-HA or GPR158- $\Delta$ C2-HA (Fig.5A). The VCPWE motifs located in the cytoplasmic domain of GPR158 were identified as key elements for the interaction with  $G\alpha_o$ , as the mutation of all 3 motifs (GPR158-

Mut4), largely decreased the TR-FRET signal with  $G\alpha_o$  (Fig.5A). While Mut1 and Mut3 show a lower TR-FRET signal than WT GPR158 with  $G\alpha_o$ , the signal with Mut2 was not affected (Fig.5A lower panel). These results revealed that motifs 1 and 3 were involved in the association of  $G\alpha_o$  with GPR158. However, the Mut1 protein level was significantly reduced compared to that of Mut3 (Fig.5A Middle panel), suggesting Mut1 is involved in a lesser extent than Mut3 in  $\alpha_o$  interaction. When using a BRET approach (Fig.5D), and to a less extent using TR-FRET approach (Fig.5A),  $G\alpha_o$  interaction with GPR158-Mut4 could still be measured, however the signal was lower than that obtained with the WT GPR158. This is consistent with the existence of a second  $G\alpha_o$  interacting site in GPR158 (Orlandi et al., 2015). The difference between the observed TR-FRET and BRET signals is likely related to photophysical properties of the techniques, as the dyes used for each technique display different  $R_o$  (5 and 10 nm, respectively). This would be further enhanced by the larger distance contributed by the size of antibodies used in the TR-FRET approach. Because GPR158 behaves as a scaffolding protein for G protein signaling proteins and can interact with G protein subunits even in absence of ligand, we then asked whether GPR158 displayed GPCR canonical basal coupling to G proteins, as described for many GPCRs (Oh et al., 2006; Thathiah et al., 2009).

### **GPR158 did not display detectable constitutive coupling to Gq, Gs, or Gi/o proteins**

To assess the putative basal G protein activation by GPR158, we used a BRET assay. This assay monitors the association state of the  $G\alpha_o:\beta\gamma$  protein complex composed of  $G\alpha_o$ -RLuc and  $\beta\gamma$ -Venus. The BRET signal decreases when a  $G_o$ -coupled GPCR is activated, as illustrated with the  $\mu$  opioid receptor (MOR) (Fig.6A) and the  $GABA_B$  receptor (Fig.6B). In contrast, the BRET signal was not affected by the vasopressin receptor V2, known not to couple to  $G_o$  (Fig.6A). In addition, a basal coupling to  $G_o$  of both MOR (Fig.6A) and  $GABA_B$  (Fig.6B) in the absence of ligand could be detected, but not for V2 (Fig.6A). Moreover, the basal  $G_o$  coupling of MOR increased as a function of MOR cell surface protein level measured using non-permeable fluorescent labeling of Snap tag domains inserted at the N-terminal end of the receptor (Fig.6C). Interestingly, increasing GPR158 expression also led to a proportional decrease of BRET signal (Fig.6C), suggesting a ligand-independent basal coupling of GPR158 to  $G_o$ .

However, this GPR158 basal coupling to G protein was not associated with any change in a second messenger production-based readout (Fig.6D), in contrast to what was observed with either MOR or GABA<sub>B</sub>. The chimeric GqTop protein containing portions of Gi/o protein was used to allow Gi/o-coupled receptors to activate PLC leading to the production of inositol monophosphate (IP1), as illustrated with MOR or GABA<sub>B</sub> (Fig.6D, Supplemental Figure 5). In contrast to the large basal increase in IP1 production measured in GABA<sub>B</sub> receptor expressing cells or to a lesser extent in MOR expressing cells, no effect was observed with GPR158 despite a similar protein level of both receptors (Fig.6D). These data bring no evidence for a constitutive canonical GqTop protein activation by GPR158, suggesting no constitutive Gi/o or Gq proteins activation either. Moreover, no detectable GPR158 constitutive coupling to Gs or Gi as assessed by the adenylyl cyclase-driven production of the second messenger cAMP (Supplemental Figure 5) could be detected.

Further analysis of GPR158 7TM amino-acid sequence identified residues K502 and R505 in TM3 (Supplemental Figure 6), highly conserved in Class C receptors from fish to human and the mutations of which (such as mutations equivalent to K502E or R505A of GPR158 in GABA<sub>B</sub> receptor) do affect the ligand-induced and constitutive activity of GABA<sub>B</sub>, mGlu1, or calcium sensing (CaS) GPCRs (Ango et al., 2001; Binet et al., 2007; Duthey et al., 2002; Francesconi and Duvoisin, 1998; Pin et al., 2004; Rondard et al., 2011). Surprisingly, the effect of GPR158 on Go activation/dissociation was not significantly altered when the receptor bore mutations K502E or R505A (Fig.7A, B). The data above showed that GPR158 affects the heterotrimeric G $\alpha$ : $\beta$  $\gamma$  association state, and that this effect is unlikely due to a ligand-independent canonical coupling to Go protein. As additional evidence in support of this conclusion, the effect of GPR158 on Go is slightly diminished after treatment with the Gi/o inhibitor Pertussis Toxin (PTX), but the PTX effect is similar to that observed with mock-transfected cells, suggesting that the effect of GPR158 on Go is PTX-independent. In contrast, both the basal and agonist-induced Go activation observed with MOR is, as expected, largely inhibited by PTX (Fig. 7C).

**GPR158 VCPWE motifs constitutively increased dissociated Go levels in cells independently to classical G protein coupling**

We found that the VCPWE motifs are essential for the GPR158 effect on Go. First, deletion of the C-terminal domain of GPR158 (GPR158- $\Delta$ C1) completely abolished the GPR158-induced change in Go BRET signal (Fig.8A). Second, the mutation of all three motifs (GPR158-Mut4) suppressed the effect of GPR158 on the Go BRET sensor (Fig.8B). However, the mutation of only one of these motifs was not sufficient to suppress the GPR158 effect (Fig.8C, D), nor the combined mutation of motifs 1 and 2 or 2 and 3 (Fig.8E, F). Indeed, only the combined mutation of both VCPWE motifs 1 and 3 led to a suppression of the GPR158 effect on the Go BRET sensor (Fig.8E).

## **Discussion**

Signaling and functions of GPR158 remain poorly characterized, although it has been proposed to be involved in the effect of Osteocalcin in the brain (Khrimian et al., 2017). The scaffolding ability of GPR158 to interact with RGS7 allows it to regulate Go signaling induced by neighboring receptors when expressed in the same cells (Orlandi et al., 2012). Besides, GPR158 binds G $\alpha$ o but its ability to couple to Go is still unclear. Furthermore, while GPR158 possesses 3 conserved VCPWE motifs, their function is still not elucidated.

Here we addressed the role of scaffolding and signaling of GPR158. We show that RGS7 interacts in the proximal part of the C-terminal intracellular domain, while G $\alpha$ o interacts downstream of this site with two of the three VCPWE motifs. Intriguingly, despite its ability to interact with G $\alpha$ o, we did not find any evidence for a canonical basal activation of this G protein by GPR158. Instead we propose that GPR158, under basal condition, can regulate Go signaling by trapping the G $\alpha$ o subunit, leaving  $\beta\gamma$  to act on its effectors. Although our data are all obtained in a recombinant system, our analysis using various expression levels of the partners, and the use of different tags, inserted at different location, and various approaches provides a good indication that what is reported here is likely also occurring in native systems. With that said, we cannot exclude that the described process can be further controlled by other partners not expressed in HEK293 cells. A possible canonical G protein activation upon agonist binding to GPR158 cannot be excluded, as this was not examined in the present study.

We delineated the RGS7 binding site in the 714-764 region of GPR158 C-terminal domain, proximal to the 7TM domain (Fig.3). This small region overlaps with the CD1 region defined by Orlandi *et al.* as containing a binding site for RGS7 (Orlandi et al., 2015) and displaying homology with R7BP protein. Indeed, GPR158 and R7BP compete for interacting with RGS7. RGS7 is composed of the RGS, GGL, and DEP domains. The latter is proposed to interact with GPR158 (Orlandi et al., 2012) as well as other proteins but no clear DEP binding consensus sequence has been identified. As observed with R7BP, GPR158 also stabilizes the RGS7 protein, leading to an increase in RGS7 protein level (Fig.4). Consistent with this observation in HEK293 cells, a decrease of RGS7 protein level has been reported in GPR158 KO mice, with diminution of the pool of RGS7 in the membrane fraction and relocation into the cytoplasm, as revealed by electron microscopy in native and transfected models (Orlandi et al., 2012, 2015). Accordingly, GPR158

appears to regulate the pool of RGS7 and tunes its localization to the plasma membrane. RGS7 protein level is also known to depend on the co-expression of  $\beta 5$  (Supplemental Figure 1)(Anderson et al., 2009), which binds to RGS7 GGL domain to form a putative G protein  $\beta\gamma$  complex. As such, RGS7 binds GPR158 and  $\beta 5$  via two independent domains, DEP and GGL respectively, leaving its RGS domain free to bind active  $G\alpha o$  and deactivate it.

We also demonstrated that two of the VCPWE motifs (motifs 1 & 3) of GPR158 were important for  $G\alpha o$  binding, even in the absence of RGS7 (Fig.5). Motif 2 in primates including human GPR158 does not contain the conserved proline residue suggesting it has lost its ability to bind  $G\alpha o$  during evolution (Supplemental Figure 2) (Slep et al., 2001). Mutation of the three motifs did not completely suppress  $G\alpha o$  binding as revealed with the BRET approach, suggesting that there might be another site. Interestingly, Orlandi et al. reported two  $G\alpha o$  binding sites in GPR158 C-terminal domain (Orlandi et al., 2015), one in close proximity to the RGS7 binding site and another one in the distal part of the C-terminal domain. Thus, according to our data, VCPWE motifs may correspond to this second distal site while the other corresponds to the proximal site. The remaining  $G\alpha o$  interaction observed after mutating the VCPWE motifs could also simply be indirect, due to a proximity to GPR158 resulting from  $G\alpha o$  association with RGS7 or other proteins/GPCRs interacting with GPR158.

We further showed that the VCPWE motifs are not only important for  $G\alpha o$  binding but also impacted  $G\alpha o:\beta\gamma$  association. The observed decreased of BRET between  $G\alpha o$ -RLuc and  $\beta\gamma$ -Venus in the presence of GPR158 (Fig.6) could reflect the dissociation or the conformational change usually observed upon G protein activation (Gales et al., 2006). However, because we obtained no evidence for a canonical activation of G proteins by GPR158 in absence of ligand, we favored alternative hypotheses. The VCPWE motifs may bind  $G\alpha o$ -RLuc, reducing its association with  $\beta\gamma$ -Venus, or  $G\alpha o$ - $\beta\gamma$  complexes activated by other endogenous GPCRs led to the release of  $G\alpha o$  that can be trapped by VCPWE motifs preventing their re-association with  $\beta\gamma$ . Both situations likely occur, as the first explanation is supported by the PTX-insensitive component of the GPR158 effect on Go BRET sensor, while the second is supported by known action of VCPWE-related motifs. Indeed, i) ICPWE motif of the  $\gamma$  subunit of the retinal PDE binds active  $\alpha$  transducin subunit (Slep et al., 2001), and ii) the distal site in GPR158 C-terminal domain has been proposed

to preferentially bind an active form of  $G\alpha_o$  (Orlandi et al., 2015). Taken together, this suggests that VCPWE motifs likely trap isolated  $G\alpha_o$  and inhibit them from activating their effectors, while leaving  $\beta\gamma$  free to activate their own effectors. GPR158 would then induce a ligand-independent signaling bias of  $\beta\gamma$  vs  $\alpha$  subunits, an effect reminiscent of the function of some group-II AGS proteins (Blumer and Lanier, 2014). Of note, two VCPWE motifs (1 & 3) are required for this effect (Fig.8), suggesting that either one  $G\alpha_o$  binds to both motif or alternatively that each motif binds one  $G\alpha_o$  independently of each other, possibly differently regulated by RGS7. Further experiments will be necessary to clarify this point. Because GPR158 associates with Cav2 calcium channel in rat brain (Muller et al., 2010) and Kv4.2 potassium channel in mouse brain (Marionneau et al., 2009) that are both regulated by  $\beta\gamma$  and RGS proteins, such a  $G\alpha_o$  trapping mechanism by the VCPWE motifs may change the kinetics of such regulatory effects of GPR158. In the retina where both RGS7 and the GPR158-related GPR179 containing 21 VCPWE motifs are expressed (Audo et al., 2012; Orlandi et al., 2012), such a mechanism could control the spatio-temporal regulation of signaling of photoreceptors and ON bipolar cells. This process may be reminiscent of the control of the PDE response by rhodopsin and transducin that involves RGS9/7 and the ICPWE motif of PDE  $\gamma$  subunit (Slep et al., 2001).

Many GPCRs display constitutive activity in absence of ligand, leading to constitutive canonical G protein coupling, and mutation-driven constitutive activity of some GPCRs leads to various diseases (Tao, 2008). GPR158 possesses Class C GPCR features required for G protein coupling (Bjarnadóttir et al., 2005), like Lysine and Arginine residues in TM3 previously shown to be important for G protein coupling in  $GABA_B$  (Binet et al., 2007; Galvez et al., 2001) and mGlu5 (Doré et al., 2014; Koehl et al., 2019). However, we did not detect any constitutive G protein activation when measuring  $G_o/i$ ,  $G_q$ , or  $G_s$  activity in HEK293 cells expressing WT or mutated GPR158. One can envisage that GPR158 displays no constitutive canonical G protein coupling, or that GPR158 couples to other pathways that have not been addressed in this work, like those resulting from G12/13 protein, or the G-independent arrestin pathway, although no direct coupling to arrestin has been clearly demonstrated for any Class C GPCRs so far (Pin and Bettler, 2016). Another possibility is that GPR158 needs a GPCR partner, like the  $GABA_B$  receptor requiring the association of two different proteins GB1 and GB2 (Pin et al., 2004; Rondard et al.,



2011). More work is needed to clarify this important issue. As already mentioned above, such data do not exclude a direct G protein activation by GPR158 upon agonist binding.

Dimer formation is required for activation of the multidomain Class C mGlu, CaS, taste T1Rs, and GABA<sub>B</sub> receptors. Indeed, the inter-subunit movement of the ECD resulting from ligand binding changes the interaction mode of the 7TM domains leading to the activation of one of them (Koehl et al., 2019; Pin and Bettler, 2016; Xue et al., 2015). We show here that GPR158 also forms homodimers, making possible a similar activation process with ligands interacting in the GPR158 ECD. However, not only does this ECD not share similarity with that of other class C GPCRs, but also with any other protein of known structure, making it impossible to perform any prediction on the mode of action of such a domain. It will be of clear importance to elucidate whether and how GPR158 can directly activate G protein upon activation with a ligand.

Not all 7TM proteins do couple to G proteins, like the adiponectin receptor (Vasiliauskaitė-Brooks et al., 2017), the GB1 subunit of GABA<sub>B</sub>, or both T1R1 and T1R2 that need to be associated with T1R3 to form the umami and sweet taste receptors, respectively (Kniazeff et al., 2011). Some orphan GPCRs are also considered to be regulatory associated proteins that control the activity of functional GPCRs, as shown elegantly for the orphan receptor GPR50 that inhibits the melatonin receptor MT1 (Levoye et al., 2006) or control TGFβ signaling (Wojciech et al., 2018). A recent article proposed that GPR158 mediates the action of the hormone Osteocalcin (Khrimian et al., 2017) which has also been reported to activate GPRC6A, another class C GPCR (Pi et al., 2005). Interestingly, in cells deleted of GPR158, Osteocalcin did not trigger an increase of BDNF expression (Khrimian et al., 2017), while the production of the second messengers IP3 was decreased, suggesting that Osteocalcin action on GPR158 modulates IP3 production. Although we did not observe any Gαq binding nor constitutive activity toward IP3 production in transfected HEK293 cells, this does not exclude a ligand-induced activation of the Gq pathway by Osteocalcin. A signaling partner protein may be missing in HEK293 cells, to allow GPR158 to couple to Gq, as illustrated by the Class C mGlu7 glutamate receptor that needs to interact with Pick1 to couple to PLC-IP3 pathway in neurons (Perroy et al., 2000). Moreover, mGlu4 reported to be Gi/o-coupled in recombinant system is endogenously coupled to the Gq pathway in parallel fiber-Purkinje cell synapses (Abitbol et al., 2012).

According to our data and previous studies, GPR158 behaves as a scaffolding platform that tunes the Go pathway in an original way. In absence of ligand, GPR158 displays various roles. First, it associates, stabilizes, and brings RGS7 to the plasma membrane where RGS7 deactivates Go proteins activated by surrounding receptors (Orlandi et al., 2012). Second, the GPR158 VCPWE motifs-mediated trapping action on G $\alpha$ o could impact the Go signaling in the surrounding microenvironment and favor  $\beta\gamma$ -mediated signaling. Third, GPR158 can be associated to both RGS7 and G $\alpha$ o leading to a complex regulation of Go pathway involving VCPWE motifs. Finally, in presence of ligand, GPR158 could couple to IP3 production via Gq as recently proposed (Khrimian et al., 2017). The integration of the signaling functions of GPR158 is a fascinating issue, as GPR158 would then control Gq pathway in a canonical way and modulate at the same time the Gi/o pathways in a completely atypical way, similarly to some group-II AGS proteins. Taken together, our data further illustrates the numerous possibilities 7TM proteins use to control cell signaling.

**Acknowledgements:**

The project has been granted by the EIDOS Collaborative team IGF-Cisbio Bioassays (Codolet, France). MH has been supported by a “Presidence PhD Grant” from University of Montpellier (France). The pharmacology, BRET, and FRET experiments have been performed using the ARPEGE Pharmacology-Screening-Interactome platform facility (UMS Biocampus), Montpellier, France. We thank Robert Healey for reading and English editing of the manuscript.

**Authorship Contribution:**

*Participated in research design:* Prézeau

*Conducted experiments:* Hajj, DeVita, Bologna, Vol, Renassia, Brabet, Cazade

*Contributed new reagents or analytical tools:* Blahos, Labesse

*Performed data analysis:* Prézeau, Hajj, DeVita, Bologna, Pastore

*Wrote the manuscript:* Prézeau and Pin

*Contributed to the writing or reading of the manuscript:* Hajj

**References:**

- Abitbol, K., McLean, H., Bessiron, T., and Daniel, H. (2012). A new signalling pathway for parallel fibre presynaptic type 4 metabotropic glutamate receptors (mGluR4) in the rat cerebellar cortex. *J. Physiol.* *590*, 2977–2994.
- Anderson, G.R., Posokhova, E., and Martemyanov, K.A. (2009). The R7 RGS protein family: multi-subunit regulators of neuronal G protein signaling. *Cell Biochem. Biophys.* *54*, 33–46.
- Ango, F., Prezeau, L., Muller, T., Tu, J.C., Xiao, B., Worley, P.F., Pin, J.P., Bockaert, J., and Fagni, L. (2001). Agonist-independent activation of metabotropic glutamate receptors by the intracellular protein Homer. *Nature* *411*, 962–965.
- Audo, I., Bujakowska, K., Orhan, E., Poloschek, C.M., Defoort-Dhellemmes, S., Drumare, I., Kohl, S., Luu, T.D., Lecompte, O., Zrenner, E., et al. (2012). Whole-exome sequencing identifies mutations in GPR179 leading to autosomal-recessive complete congenital stationary night blindness. *Am. J. Hum. Genet.* *90*, 321–330.
- Ayoub, M.A., Maurel, D., Binet, V., Fink, M., Prezeau, L., Ansanay, H., and Pin, J.P. (2007). Real-time analysis of agonist-induced activation of protease-activated receptor 1/Gα<sub>q</sub> protein complex measured by bioluminescence resonance energy transfer in living cells. *Mol Pharmacol* *71*, 1329–1340.
- Binet, V., Duthey, B., Lecaillon, J., Vol, C., Quoyer, J., Labesse, G., Pin, J.P., and Prezeau, L. (2007). Common structural requirements for heptahelical domain function in class A and class C G protein-coupled receptors. *J Biol Chem* *282*, 12154–12163.
- Bjarnadóttir, T.K., Schiöth, H.B., and Fredriksson, R. (2005). The phylogenetic relationship of the glutamate and pheromone G-protein-coupled receptors in different vertebrate species. *Ann. N. Y. Acad. Sci.* *1040*, 230–233.
- Blumer, J.B., and Lanier, S.M. (2014). Activators of G protein signaling exhibit broad functionality and define a distinct core signaling triad. *Mol. Pharmacol.* *85*, 388–396.
- Bockaert, J., Perroy, J., Becamel, C., Marin, P., and Fagni, L. (2010). GPCR interacting proteins (GIPs) in the nervous system: Roles in physiology and pathologies. *Annu Rev Pharmacol Toxicol* *50*, 89–109.
- Brulé, C., Perzo, N., Joubert, J.-E., Sainsily, X., Leduc, R., Castel, H., and Prézeau, L. (2014). Biased signaling regulates the pleiotropic effects of the urotensin II receptor to modulate its cellular behaviors. *FASEB J. Off. Publ. Fed. Am. Soc. Exp. Biol.* *28*, 5148–5162.
- Condomitti, G., Wierda, K.D., Schroeder, A., Rubio, S.E., Vennekens, K.M., Orlandi, C., Martemyanov, K.A., Goukko, N.V., Savas, J.N., and de Wit, J. (2018). An Input-Specific Orphan Receptor GPR158-HSPG Interaction Organizes Hippocampal Mossy Fiber-CA3 Synapses. *Neuron* *100*, 201–215.e9.
- Doré, A.S., Okrasa, K., Patel, J.C., Serrano-Vega, M., Bennett, K., Cooke, R.M., Errey, J.C., Jazayeri, A., Khan, S., Tehan, B., et al. (2014). Structure of class C GPCR metabotropic glutamate receptor 5 transmembrane domain. *Nature* *511*, 557–562.
- Doumazane, E., Scholler, P., Zwier, J.M., Trinquet, E., Rondard, P., and Pin, J.-P. (2011). A new approach to analyze cell surface protein complexes reveals specific heterodimeric metabotropic glutamate receptors. *FASEB J.* *25*, 66–77.
- Duthey, B., Caudron, S., Perroy, J., Bettler, B., Fagni, L., Pin, J.P., and Prezeau, L. (2002). A single subunit (GB2) is required for G-protein activation by the heterodimeric GABA(B) receptor. *J Biol Chem* *277*, 3236–3241.
- El Moustaine, D., Granier, S., Doumazane, E., Scholler, P., Rahmeh, R., Bron, P., Mouillac, B.,

- Banères, J.-L., Rondard, P., and Pin, J.-P. (2012). Distinct roles of metabotropic glutamate receptor dimerization in agonist activation and G-protein coupling. *Proc. Natl. Acad. Sci. U. S. A.* *109*, 16342–16347.
- Francesconi, A., and Duvoisin, R.M. (1998). Role of the second and third intracellular loops of metabotropic glutamate receptors in mediating dual signal transduction activation. *J Biol Chem* *273*, 5615–5624.
- Gales, C., Van Durm, J.J., Schaak, S., Pontier, S., Percherancier, Y., Audet, M., Paris, H., and Bouvier, M. (2006). Probing the activation-promoted structural rearrangements in preassembled receptor-G protein complexes. *Nat Struct Mol Biol* *13*, 778–786.
- Galvez, T., Duthey, B., Kniazeff, J., Blahos, J., Rovelli, G., Bettler, B., Prezeau, L., and Pin, J.P. (2001). Allosteric interactions between GB1 and GB2 subunits are required for optimal GABA(B) receptor function. *Embo J* *20*, 2152–2159.
- Gerber, K.J., Squires, K.E., and Hepler, J.R. (2016). Roles for Regulator of G Protein Signaling Proteins in Synaptic Signaling and Plasticity. *Mol. Pharmacol.* *89*, 273–286.
- Greif, P.A., Yaghmaie, M., Konstandin, N.P., Ksienzyk, B., Alimoghaddam, K., Ghavamzadeh, A., Hauser, A., Graf, A., Krebs, S., Blum, H., et al. (2011). Somatic mutations in acute promyelocytic leukemia (APL) identified by exome sequencing. *Leukemia* *25*, 1519–1522.
- Khrimian, L., Obri, A., Ramos-Brossier, M., Rousseaud, A., Moriceau, S., Nicot, A.-S., Mera, P., Kosmidis, S., Karnavas, T., Saudou, F., et al. (2017). Gpr158 mediates osteocalcin's regulation of cognition. *J. Exp. Med.* *214*, 2859–2873.
- Kniazeff, J., Saintot, P.-P., Goudet, C., Liu, J., Charnet, A., Guillon, G., and Pin, J.-P. (2004). Locking the dimeric GABAB G-protein coupled receptor in its active state. *J Neurosci.* *24*, 370–377.
- Kniazeff, J., Prézeau, L., Rondard, P., Pin, J.-P., and Goudet, C. (2011). Dimers and beyond: The functional puzzles of class C GPCRs. *Pharmacol. Ther.* *130*, 9–25.
- Koehl, A., Hu, H., Feng, D., Sun, B., Zhang, Y., Robertson, M.J., Chu, M., Kobilka, T.S., Laeremans, T., Steyaert, J., et al. (2019). Structural insights into the activation of metabotropic glutamate receptors. *Nature* *566*, 79–84.
- Levoye, A., Dam, J., Ayoub, M.A., Guillaume, J.L., Couturier, C., Delagrangé, P., and Jockers, R. (2006). The orphan GPR50 receptor specifically inhibits MT1 melatonin receptor function through heterodimerization. *Embo J* *25*, 3012–3023.
- Marionneau, C., LeDuc, R.D., Rohrs, H.W., Link, A.J., Townsend, R.R., and Nerbonne, J.M. (2009). Proteomic analyses of native brain K(V)4.2 channel complexes. *Channels Austin Tex* *3*, 284–294.
- Maurel, D., Kniazeff, J., Mathis, G., Trinquet, E., Pin, J.P., and Ansanay, H. (2004). Cell surface detection of membrane protein interaction with homogeneous time-resolved fluorescence resonance energy transfer technology. *Anal Biochem* *329*, 253–262.
- Maurel, D., Comps-Agrar, L., Brock, C., Rives, M.L., Bourrier, E., Ayoub, M.A., Bazin, H., Tinel, N., Durroux, T., Prezeau, L., et al. (2008). Cell-surface protein-protein interaction analysis with time-resolved FRET and snap-tag technologies: application to GPCR oligomerization. *Nat Methods* *5*, 561–567.
- Milligan, G. (2006). G-protein-coupled receptor heterodimers: pharmacology, function and relevance to drug discovery. *Drug Discov Today* *11*, 541–549.
- Muller, C.S., Haupt, A., Bildl, W., Schindler, J., Knaus, H.G., Meissner, M., Rammner, B., Striessnig, J., Flockerzi, V., Fakler, B., et al. (2010). Quantitative proteomics of the Cav2 channel nano-environments in the mammalian brain. *Proc Natl Acad Sci U A* *107*, 14950–

14957.

- Oh, D.Y., Kim, K., Kwon, H.B., and Seong, J.Y. (2006). Cellular and molecular biology of orphan G protein-coupled receptors. *Int Rev Cytol* 252, 163–218.
- Orlandi, C., Posokhova, E., Masuho, I., Ray, T.A., Hasan, N., Gregg, R.G., and Martemyanov, K.A. (2012). GPR158/179 regulate G protein signaling by controlling localization and activity of the RGS7 complexes. *J. Cell Biol.* 197, 711–719.
- Orlandi, C., Xie, K., Masuho, I., Fajardo-Serrano, A., Lujan, R., and Martemyanov, K.A. (2015). Orphan Receptor GPR158 Is an Allosteric Modulator of RGS7 Catalytic Activity with an Essential Role in Dictating Its Expression and Localization in the Brain. *J. Biol. Chem.* 290, 13622–13639.
- Overington, J.P., Al-Lazikani, B., and Hopkins, A.L. (2006). How many drug targets are there? *Nat Rev Drug Discov* 5, 993–996.
- Patel, N., Itakura, T., Gonzalez, J.M., Schwartz, S.G., and Fini, M.E. (2013). GPR158, an Orphan Member of G Protein-Coupled Receptor Family C: Glucocorticoid-Stimulated Expression and Novel Nuclear Role. *PLoS ONE* 8, e57843.
- Patel, N., Itakura, T., Jeong, S., Liao, C.-P., Roy-Burman, P., Zandi, E., Groshen, S., Pinski, J., Coetzee, G.A., Gross, M.E., et al. (2015). Expression and Functional Role of Orphan Receptor GPR158 in Prostate Cancer Growth and Progression. *PLOS ONE* 10, e0117758.
- Perroy, J., Prezeau, L., De Waard, M., Shigemoto, R., Bockaert, J., and Fagni, L. (2000). Selective blockade of P/Q-type calcium channels by the metabotropic glutamate receptor type 7 involves a phospholipase C pathway in neurons [In Process Citation]. *J Neurosci* 20, 7896–7904.
- Pi, M., Faber, P., Ekema, G., Jackson, P.D., Ting, A., Wang, N., Fontilla-Poole, M., Mays, R.W., Brunden, K.R., Harrington, J.J., et al. (2005). Identification of a novel extracellular cation-sensing G-protein-coupled receptor. *J Biol Chem* 280, 40201–40209.
- Pin, J.-P., and Bettler, B. (2016). Organization and functions of mGlu and GABAB receptor complexes. *Nature* 540, 60–68.
- Pin, J.P., Kniazeff, J., Goudet, C., Bessis, A.S., Liu, J., Galvez, T., Acher, F., Rondard, P., and Prezeau, L. (2004). The activation mechanism of class-C G-protein coupled receptors. *Biol Cell* 96, 335–342.
- Prezeau, L., Rives, M.L., Comps-Agrar, L., Maurel, D., Kniazeff, J., and Pin, J.P. (2010). Functional crosstalk between GPCRs: with or without oligomerization. *Curr Opin Pharmacol* 10, 6–13.
- Rives, M.L., Vol, C., Fukazawa, Y., Tinel, N., Trinquet, E., Ayoub, M.A., Shigemoto, R., Pin, J.P., and Prezeau, L. (2009). Crosstalk between GABA(B) and mGlu1a receptors reveals new insight into GPCR signal integration. *Embo J* 28, 2195–2208.
- Rondard, P., Goudet, C., Kniazeff, J., Pin, J.P., and Prezeau, L. (2011). The complexity of their activation mechanism opens new possibilities for the modulation of mGlu and GABAB class C G protein-coupled receptors. *Neuropharmacology* 60, 82–92.
- Slep, K.C., Kercher, M.A., He, W., Cowan, C.W., Wensel, T.G., and Sigler, P.B. (2001). Structural determinants for regulation of phosphodiesterase by a G protein at 2.0 Å. *Nature* 409, 1071–1077.
- Tao, Y.X. (2008). Constitutive activation of G protein-coupled receptors and diseases: insights into mechanisms of activation and therapeutics. *Pharmacol Ther* 120, 129–148.
- Thathiah, A., Spittaels, K., Hoffmann, M., Staes, M., Cohen, A., Horr , K., Vanbrabant, M., Coun, F., Baekelandt, V., Delacourte, A., et al. (2009). The orphan G protein-coupled

- receptor 3 modulates amyloid-beta peptide generation in neurons. *Science* 323, 946–951.
- Vasiliauskaitė-Brooks, I., Sounier, R., Rochaix, P., Bellot, G., Fortier, M., Hoh, F., De Colibus, L., Bechara, C., Saied, E.M., Arenz, C., et al. (2017). Structural insights into adiponectin receptors suggest ceramidase activity. *Nature* 544, 120–123.
- Wojciech, S., Ahmad, R., Belaid-Choucair, Z., Journé, A.-S., Gallet, S., Dam, J., Daulat, A., Ndiaye-Lobry, D., Lahuna, O., Karamitri, A., et al. (2018). The orphan GPR50 receptor promotes constitutive TGF $\beta$  receptor signaling and protects against cancer development. *Nat. Commun.* 9, 1216.
- Wood, L.D., Parsons, D.W., Jones, S., Lin, J., Sjöblom, T., Leary, R.J., Shen, D., Boca, S.M., Barber, T., Ptak, J., et al. (2007). The genomic landscapes of human breast and colorectal cancers. *Science* 318, 1108–1113.
- Xue, L., Rovira, X., Scholler, P., Zhao, H., Liu, J., Pin, J.-P., and Rondard, P. (2015). Major ligand-induced rearrangement of the heptahelical domain interface in a GPCR dimer. *Nat. Chem. Biol.* 11, 134–140.



**Footnotes:**

- Financial support: University of Montpellier through a “Presidence PhD Grant” for financial support of Mariana Hajj’s PhD training period.

## Legends

**Figure 1: GPR158 forms dimers at the cell surface.** **A.** Western blot analysis using three different commercially available antibodies, recognizing the Flag epitope (M2 clone), the N-terminal (Anti N-term, SAB4502509 Sigma), or the C-terminal domain (Anti C-term, HPA013185 Sigma) of N-terminal Flag-tagged GPR158 (Flag-GPR158), revealed two major bands, at around 150 kDa and 300 kDa, in HEK293 cells transiently expressing Flag-GPR158 (+), but not in mock transfected cells (-). **B.** Co-immunoprecipitation of Flag- and HA-GPR158 co-expressed in HEK293 cells. Note that HA-GPR158 did not co-immunoprecipitate with N-terminal tagged Flag-mGlu2 or Flag-GB2 (GABA<sub>B</sub>2), while a positive control showed a co-immunoprecipitation between the two subunits Flag-GB1a and HA-GB2 of the dimeric GABA<sub>B</sub> receptor. **C.** TR-FRET analysis of GPR158 dimerization. A TR-FRET signal was recorded between Flag- and HA-GPR158, using TR-FRET donor and acceptor fluorophores labeled anti-Flag and anti-HA antibodies. Similarly, a strong TR-FRET signal was obtained between the two subunits of GABA<sub>B</sub> receptor HA-GB1a and Flag-GB2. However, no HA-Flag TR-FRET signal was detected in cells expressing Flag-GPR158 and HA-GB2. **D.** HA-GPR158 but not HA-GB2 can dimerize with Flag-GPR158. In cells expressing a constant level of Flag-GPR158, the Flag-HA TR-FRET signal increased when increasing the amount of HA-GPR158 up to saturation, in contrast to HA-GB2 increasing expression. **E.** HA-GPR158 but not HA-GB2 competed for dimerization with Flag-GPR158. In cells expressing a constant amount of Flag-GPR158, an increasing amount of HA-GPR158 decreased Flag-Flag TR-FRET signal indicating a competition in the dimer formation between the Flag- and the HA- versions of GPR158, while no competition was observed when co-expressing increasing amount of HA-GB2. In **A**, **B**, and **C** panels data are representative of three independent experiments. In panels **D** and **E**, data from three independent experiments are pooled. Data are means  $\pm$  sem of triplicate determinations. ECD, 7TM, N- and C-terminal stand for Extracellular Domain, 7 transmembrane Domain, and N- and C-terminal Domain, respectively.

**Figure 2: GPR158 C-terminal domain is required for RGS7 interaction.** **A.** C-terminal HA-tagged RGS7 (RGS7-HA) but not the C-terminal tagged RGS4 (RGS4-HA) was co-immunoprecipitated by Flag-GPR158 when co-expressed in HEK293 cells. **B.** Flag-GPR158 but

not Flag-GB2 was co-immunoprecipitated with RGS7-HA in transfected HEK293 cells. **C.** Schematic representation of the WT and truncated  $\Delta C1$  and  $\Delta C2$  (with the last residues mentioned) versions of GPR158 receptor. **D-F.** RGS7 binds to the C-terminal domain of GPR158, as shown with co-immunoprecipitation (**D, E**) and TR-FRET (**F**) approaches. HEK293 cells were transfected with WT or C-terminal domain truncated versions  $\Delta C1$  and  $\Delta C2$  of GPR158 together with RGS7 and  $\beta 5$ . In **D.**, the co-immunoprecipitation was performed using the C-terminal Flag-tagged versions of the WT (GPR158-Flag) and truncated (GPR158- $\Delta C1$ -Flag, GPR158- $\Delta C2$ -Flag) GPR158 receptor, co-expressed in HEK293 cells with RGS7-HA. In **E.**, the co-immunoprecipitation was performed using HA-GPR158 or HA-GPR158- $\Delta C1$ , co-expressed in HEK293 cells with the C-terminal Flag-tagged RGS7 (RGS7-Flag). **F.** For TR-FRET experiments, HEK293 cells expressing truncated or WT GPR158-Flag and RGS7-HA were permeabilized with tritonX-100 (0.1%) and incubated with antibodies against HA and Flag epitopes bearing the donor and acceptor fluorophores. Each experiment shown is representative of four independent experiments and data in **F** are the mean  $\pm$  sem of triplicates.

**Figure 3: RGS7 interaction requires a short region of the proximal C-terminal domain but not the VCPWE motifs.** **A.** Schematic representation of the WT and mutated forms of GPR158 used for co-immunoprecipitation (**B**) and TR-FRET (**C**) experiments. **B.** Co-immunoprecipitation was performed from cells expressing WT,  $\Delta C1$ , or mutated Mut1-4 GPR158-HA receptor together with RGS7-Flag and  $\beta 5$ . **C.** For TR-FRET experiments, HEK293 cells expressing WT,  $\Delta C1$ , Mut1, Mut2, Mut3, or Mut4 GPR158-HA together with either RGS7-Flag and  $\beta 5$  or Flag- $\beta$ -arrestin 1, were permeabilized with tritonX-100 (0.1%). The cells were then incubated with antibodies against HA and Flag epitopes bearing the donor and acceptor fluorophores. Arrestin was used as a negative control for interaction with GPR158. **D.** Last residues of the truncated versions ( $\Delta C1$ - $\Delta C11$ ) of GPR158. Co-immunoprecipitation (**E**) and TR-FRET experiments (**F**) were performed from cells co-expressing WT or truncated ( $\Delta C1$ - $\Delta C11$ ) GPR158-Flag together with RGS7-HA and  $\beta 5$  (**E, F**) or HA- $\beta$ -arrestin (**F**). Each experiment is representative of three independent experiments, and the data in **C & F** are the mean  $\pm$  sem of triplicates.

**Figure 4: RGS7 protein level is stabilized when co-expressed with GPR158.** HEK293 cells were transfected with constant amounts of plasmids coding for RGS7-HA (150ng) and  $\beta 5$  (30ng), and increasing amounts of plasmids coding for Flag-GPR158 or Flag-mGlu2 receptors (1 to 50ng) (**A**), or Flag-GPR158 or Flag-GPR158- $\Delta C1$  (1 to 50ng) (**B**). The abundance of HA-RGS7 protein was analyzed using Western blot analysis using an anti HA antibody. The tubulin protein abundance was used as a Western blot loading control. Each experiment is representative of three independent experiments.

**Figure 5: G $\alpha$ o association with GPR158 involves the VCPWE motifs.** **A.** TR-FRET-based analysis of GPR158 and G $\alpha$ o (G $\alpha$ oA isoform) association in HEK293 was measured in cells transfected with G $\alpha$ o-Flag and either the WT,  $\Delta C1$ ,  $\Delta C2$ , or Mut1-4 GPR158-HA (lower panel). The amount of G $\alpha$ o-Flag and GPR158-HA versions were quantified by ELISA (upper and middle panels, respectively) against the Flag and HA epitopes, and expressed as % of either G $\alpha$ o-Flag or WT GPR158-HA protein levels detected in the G $\alpha$ o-Flag or GPR158-HA control conditions (black bars). The amount of the G $\alpha$ o-Flag protein is not significantly different ( $p=ns$ ) in the various tested conditions (upper panel). Similarly, no significant difference was observed between the amount of the various GPR158 protein versions (middle panel), excepted between Mut1 and Mut3 versions (\* on the graph,  $p=0.0185$ ). Statistical analysis of the HTRF<sup>®</sup> signal is indicated directly on the lower panel graph. For each of the three panels, data from 6 experiments are pooled on the same graph and values are mean  $\pm$  sem. Data statistics were analyzed using a one-way ANOVA test (no difference of the variance was checked with a Brown-Forsythe method), and a multiple comparison correction was performed by Dunnett method and the adjusted  $p$ -values are reported, with  $ns=$  non-significant difference,  $*=p<0.05$ , and  $**=p<0.01$ . **B.** Interaction of GPR158 with G $\alpha$ o (G $\alpha$ oA isoform) was assessed by BRET assay in HEK293 cells transfected with G $\alpha$ o-RLuc or Homer3-RLuc and increasing amounts of GPR158-Venus. Only the association GPR158-Venus and G $\alpha$ o-RLuc generated a saturating curve suggesting a specific association. Protein levels of GPR158 and G $\alpha$  or Homer3 were monitored by determination of the specific Venus Fluorescence and RLuc Luminescence signals, the ratios of which being used for plotting the x axis. **C.** Selective association of GPR158 with various G $\alpha$  subunits. The BRET signal was monitored in cells expressing G $\alpha$ oA-RLuc, G $\alpha$ i1-RLuc, or G $\alpha$ q-RLuc and increasing amounts of GPR158-Venus.

Protein levels of GPR158 and G $\alpha$  were monitored by determination of the specific Venus Fluorescence and RLuc Luminescence signals, the ratios of which being used for plotting the x axis. **D.** BRET saturation curves have been established from cells transfected with increasing amounts of plasmids coding for WT GPR158-Venus or GPR158-Mut4-Venus and constant amounts of  $\alpha$ -RLuc. The data of three independent experiments were pooled for BRET experiments in **B**, **C**, and **D**, and values are means  $\pm$  sem of triplicate determinations.

**Figure 6: Constitutive action of GPR158 on Go.** **A & B.** HEK293 cells were transfected with plasmids coding for G $\alpha$ -Rluc,  $\beta$ 1 and  $\gamma$ 2-YFP subunits and for Snap-tagged  $\mu$  opioid (MOR) or Vasopressin V2 (V2) (**A**), or GABA $_B$  (**B**) receptors. The heterotrimeric G $\alpha$ -Rluc: $\beta\gamma$ -YFP generates a high BRET signal, which decreases in a dose-dependent manner upon increasing concentration of receptor agonist (DAMGO and GABA for MOR and GABA $_B$  receptors, respectively). In contrast, activation of the Gs-coupled receptor V2 did not affect the G $\alpha$ -Rluc: $\beta\gamma$ -YFP BRET signal. Of note, MOR (**A.**) and GABA $_B$  (**B.**) expressing cells displayed a high basal effect on G $\alpha$ -Rluc: $\beta\gamma$ -YFP BRET signal in absence of ligand compared to BRET signal detected in mock cells, indicating a constitutive coupling toward Go. **C.** As observed with increasing MOR amounts in absence of ligand, increasing levels of GPR158 affected the basal G $\alpha$ -Rluc: $\beta\gamma$ -YFP BRET signal in transfected HEK293 cells suggesting a basal effect of GRP158 on Go. In contrast, presence of V2 did not impact the BRET signal. The difference between slopes was significant as illustrated by the adjusted p-values: GPR158 vs V2, p=0.0073; GPR158 vs MOR, p=0.0002. **A-C**, each experiment is representative of three independent experiments. **D.** IP1-3 second messenger production measured in cells expressing GqTop and increasing levels of GPR158, MOR, or GABA $_B$  under basal or agonist activation (DAMGO 1  $\mu$ M, and GABA 100  $\mu$ M, for MOR and GABA $_B$ , respectively). GqTop is a chimeric G protein that allows Gi/o-coupled GPCRs to couple to Gq and the production of IP1-3 second messenger, the production of which was monitored using a HTRF®-IPOne assay. The difference between slopes is significant: GPR158 vs MOR/Basal, p=0.0003. Three experiments performed in triplicates were pooled. **C-D:** Data statistics were

analyzed using comparison of linear regression slopes, then a multiple comparison correction was performed by Benjamini-Hochberg method, and the adjusted p-values are reported.

**Figure 7: GPR158 mediated decrease in  $G\alpha o$ -Rluc: $\beta\gamma$ -YFP BRET signal is unlikely due to a canonical activation of Go.** **A.** and **B.**  $G\alpha o$ -Rluc: $\beta\gamma$ -YFP BRET signal as a function of increasing amount of V2 vasopressin (V2),  $\mu$  Opioid (MOR), WT or mutated K502E (**A**) or R505A (**B**) GPR158. **A.** There is no significant difference between slopes of GPR158 and GPR158 K502E ( $p=0.2379$ ), while the difference is significant for GPR158 vs V2 ( $p=0.0222$ ) and GPR158 K502E vs V2 ( $p=0.0379$ ). **B.** There is no significant difference between slopes of GPR158 and GPR158 R505A ( $p=0.7786$ ), while the difference is significant for GPR158 vs V2 ( $p=0.0219$ ) and GPR158 R505A vs V2 ( $p=0.0231$ ). These experiments are representative of three independent experiments. **A & B.** Data statistics were analyzed using comparison of linear regression slopes, then a multiple comparison correction was performed by Benjamini-Hochberg method, and the adjusted p-values are reported. **C.**  $G\alpha o$ -Rluc: $\beta\gamma$ -YFP BRET signal was measured in mock transfected cells or cells expressing MOR (basal or with application of DAMGO), GPR158 or GPR158-Mut4, under control condition (white bars) or after overnight PTX treatment (100 ng/mL, grey bars). Data are means  $\pm$  SD of for experiments performed in triplicates and pooled. Data statistics were analyzed using a one-way ANOVA test (variance was checked with a Brown-Forsythe method), a multiple comparison correction was then performed by Tukey's method, and the adjusted p-values are reported, with ns= non-significant difference, \*\*\*= $p<0.005$ , \*\*\*\*= $p<0.001$ ,

**Figure 8: Mutation of both VCPWE motifs 1 & 3 is required for suppressing GPR158 constitutive action on Go.** Variation of  $G\alpha o$ -Rluc: $\beta\gamma$ -YFP BRET signal was measured in HEK293 cells expressing increasing amount of V2, MOR, WT GPR158 (**A-F**), or GPR158- $\Delta$ C1 (**A**), -Mut4 (**B**), -Mut1 or -Mut2 (**C**), -Mut3 (**D**), or the double mutated GPR158-Mut1/3 or -Mut1/2 (**E**), or -Mut2/3 (**F**). **A.** There is no significant difference between slopes of GPR158  $\Delta$ C1 and V2 ( $p=0.0772$ ), while the difference is significant for GPR158 vs V2 ( $p=0.0024$ ) and GPR158 vs GPR158- $\Delta$ C1 ( $p=0.0009$ ). **B.** There is no significant difference between slopes of GPR158-Mut4 and V2 ( $p=0.3184$ ), while the difference is significant for GPR158 vs V2 ( $p=0.0018$ ) and GPR158

vs GPR158-Mut4 ( $p=0.0003$ ). **C.** There is no significant difference between slopes of GPR158 and GPR158-Mut1 ( $p=0.3096$ ) and GPR158 and GPR158-Mut2 ( $p=0.4424$ ), while the difference is significant for GPR158 vs V2 ( $p=0.0093$ ), GPR158-Mut1 vs V2 ( $p=0.0067$ ), and GPR158-Mut2 vs V2 ( $p=0.0067$ ). **D.** There is no significant difference between slopes of GPR158 and GPR158-Mut3 ( $p=0.2603$ ), while the difference is significant for GPR158 vs V2 ( $p=0.0111$ ), and GPR158-Mut3 vs V2 ( $p=0.0111$ ). **E.** There is no significant difference between slopes of GPR158 and GPR158-Mut1/2 ( $p=0.9535$ ) and GPR158-Mut1/3 vs V2 ( $p=0.9922$ ), while the difference is significant for GPR158 vs V2 ( $p=0.0036$ ) and GPR158 vs GPR158-Mut1/3 ( $p=0.0036$ ). **F.** There is no significant difference between slopes of GPR158 and GPR158-Mut2/3 ( $p=0.3456$ ), while the difference is significant for GPR158 vs V2 ( $p=0.0015$ ) and GPR158-Mut2/3 and V2 ( $p=0.0051$ ). These experiments are representative of three to four independent experiments. Data statistics were analyzed using comparison of linear regression slopes, then a multiple comparison correction was performed by Benjamini-Hochberg method, and the adjusted p-values are reported.

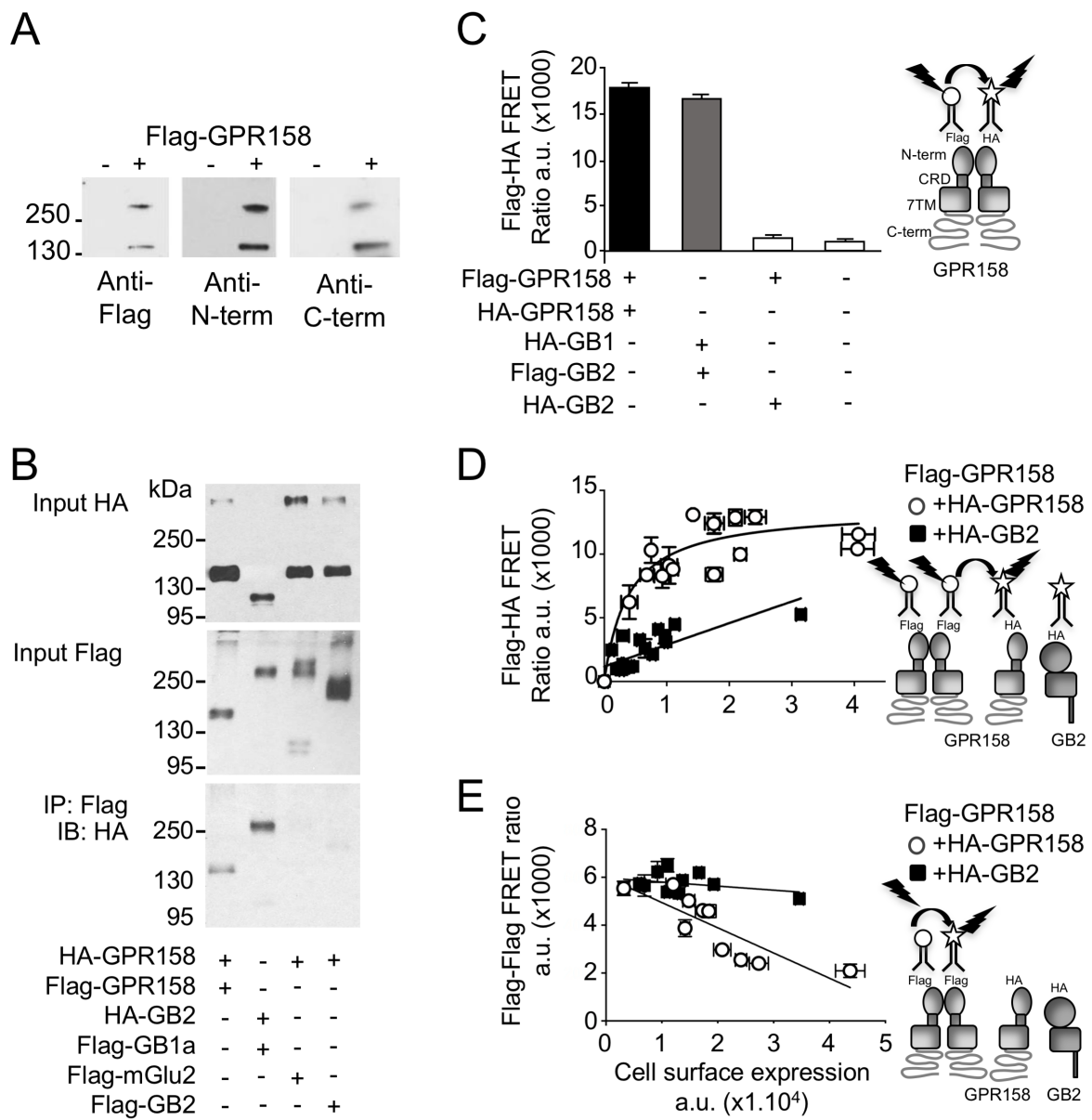


Figure 1



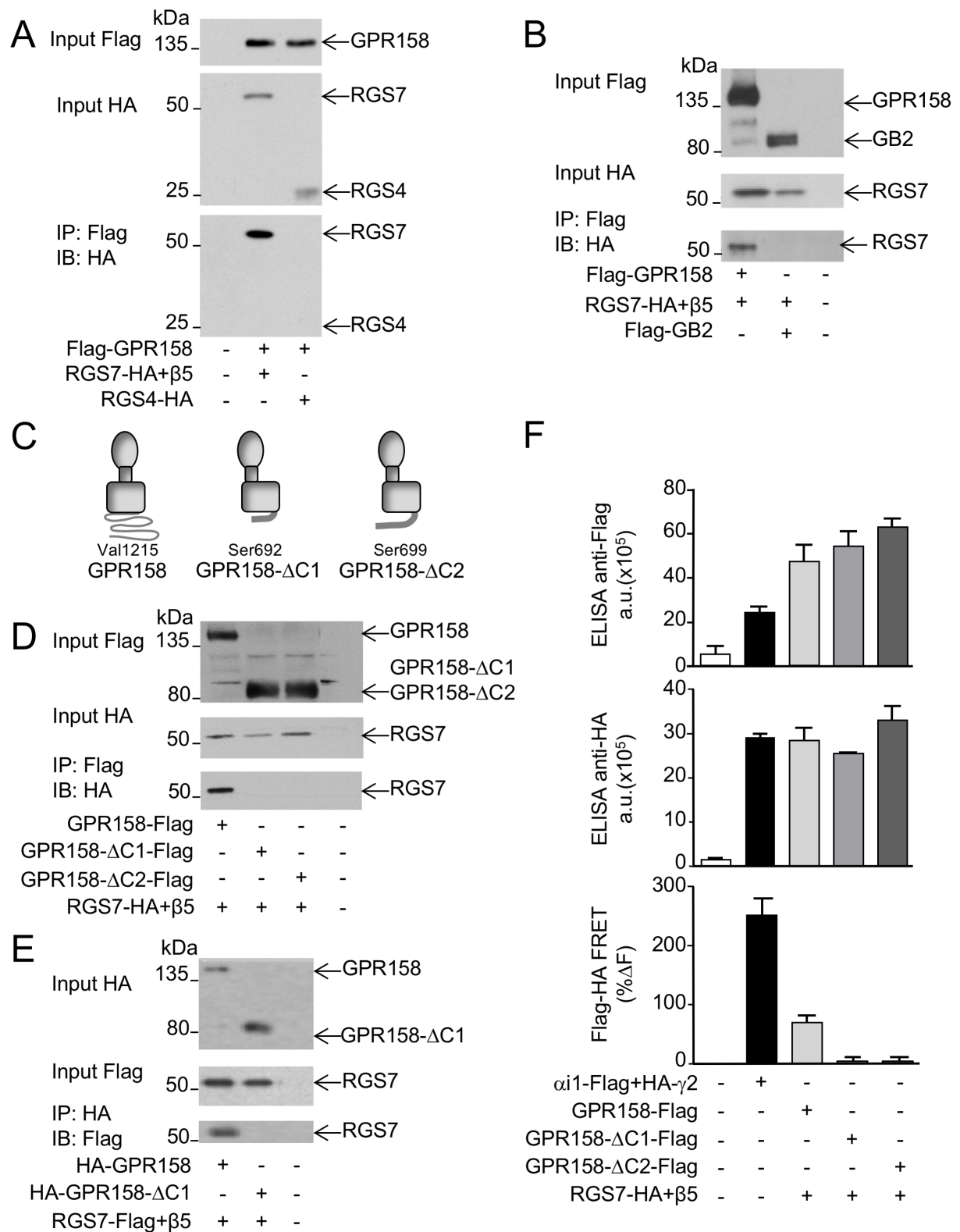


Figure 2

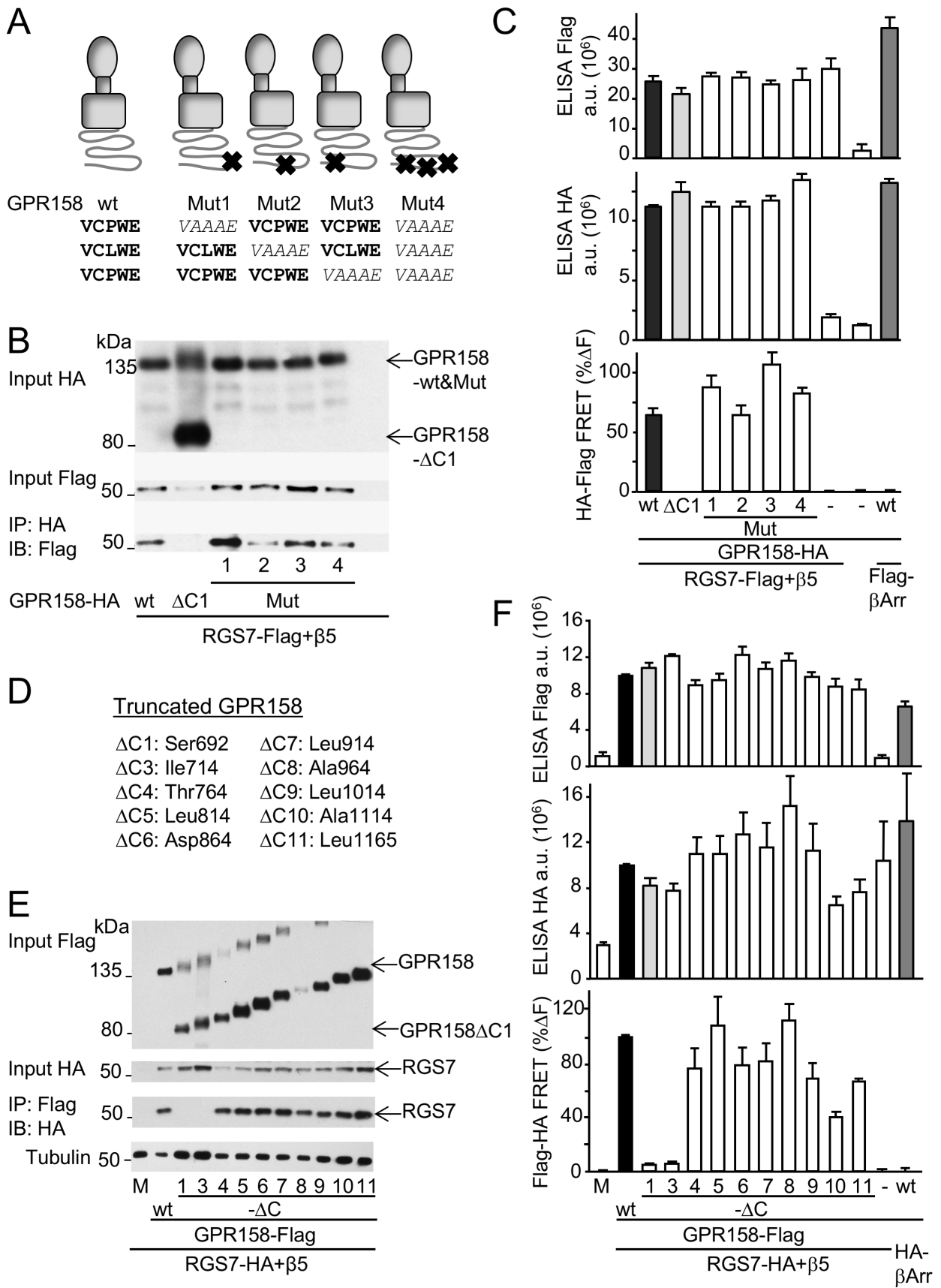


Figure 3

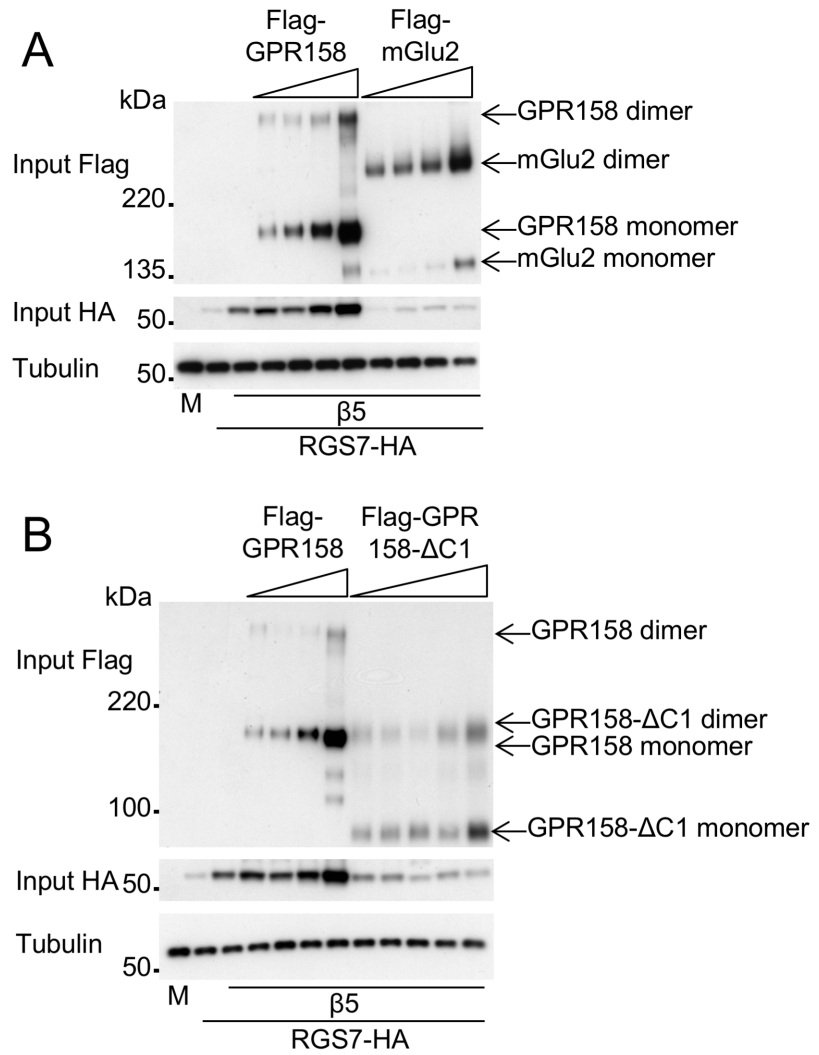


Figure 4

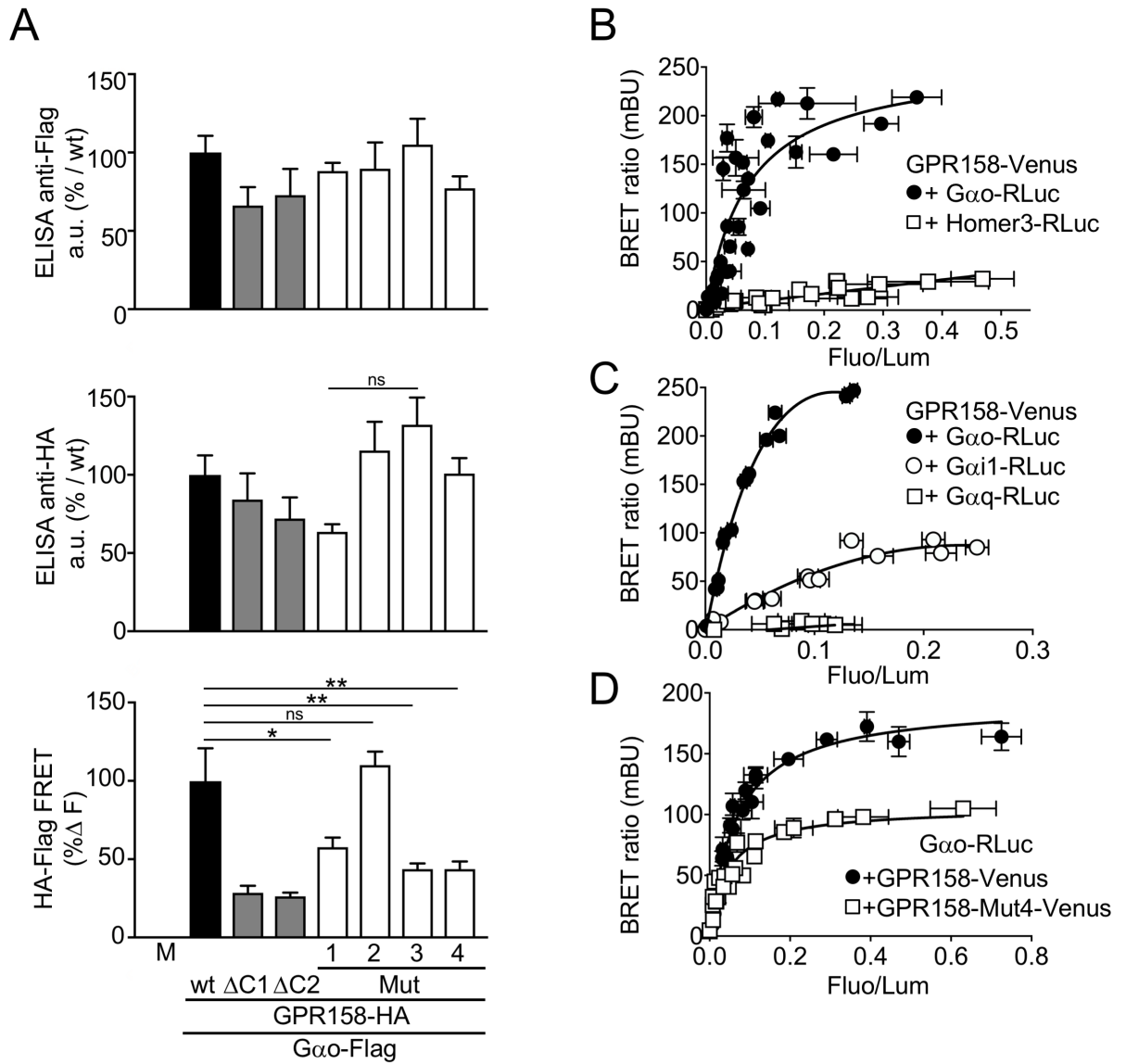


Figure 5

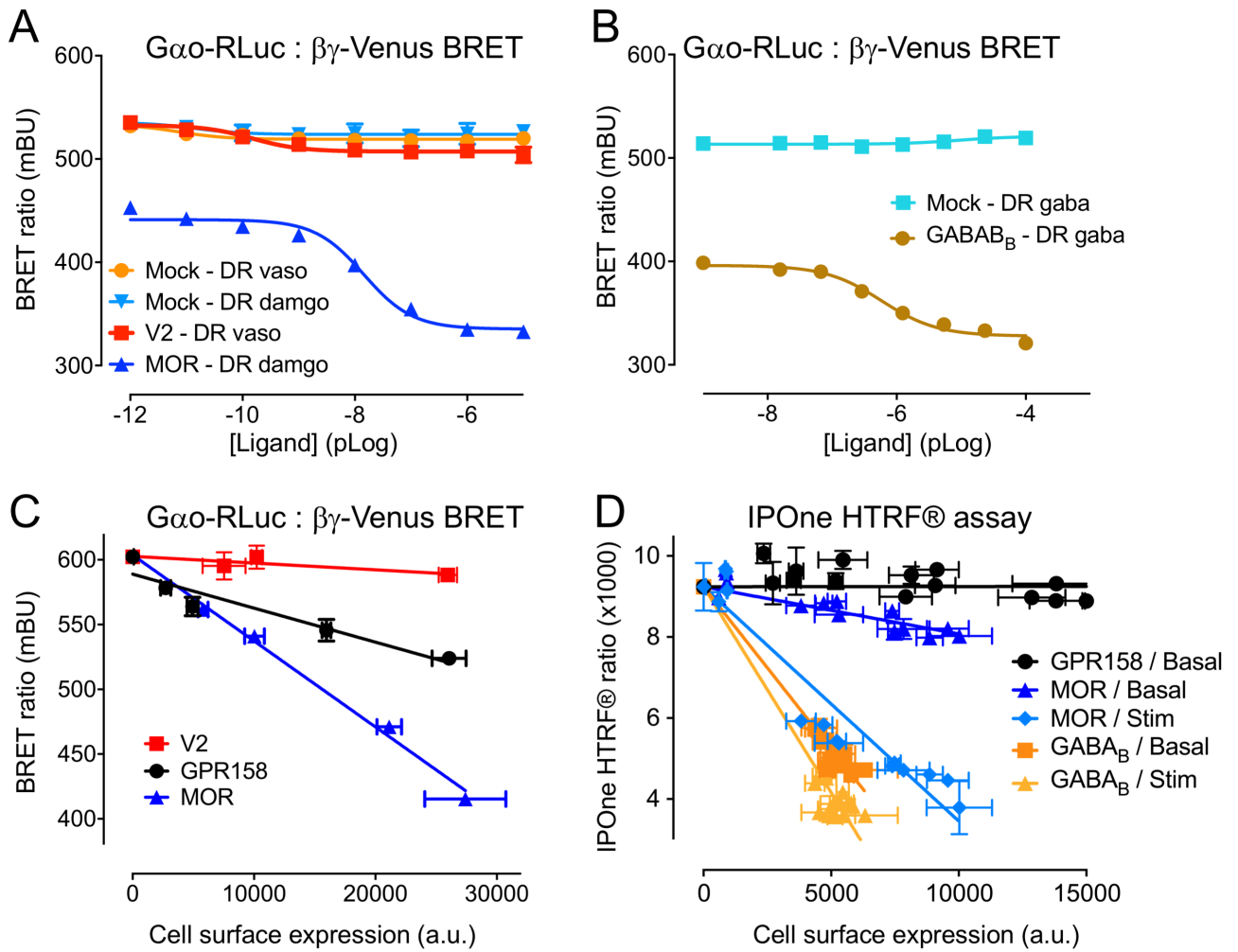


Figure 6

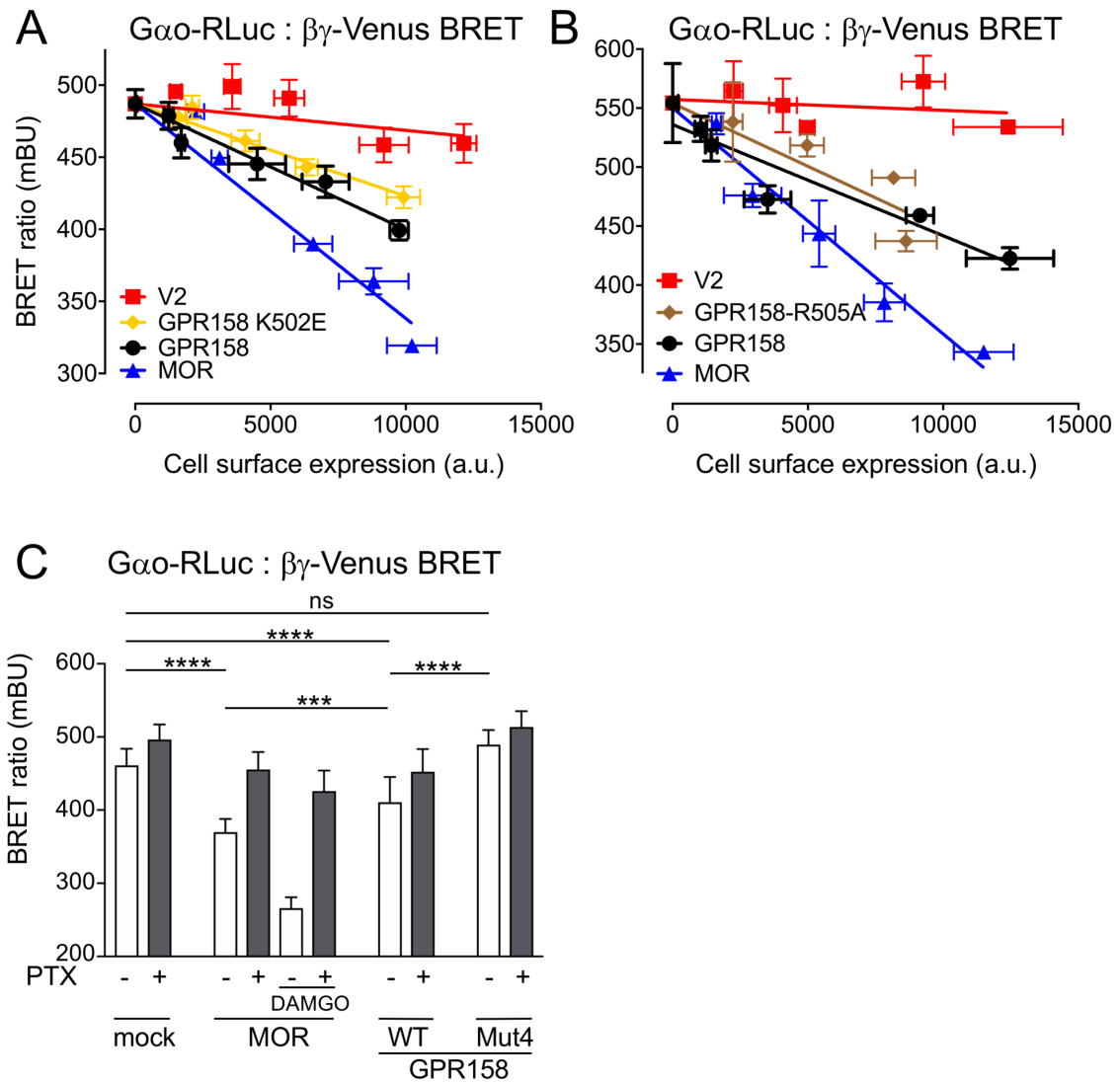


Figure 7

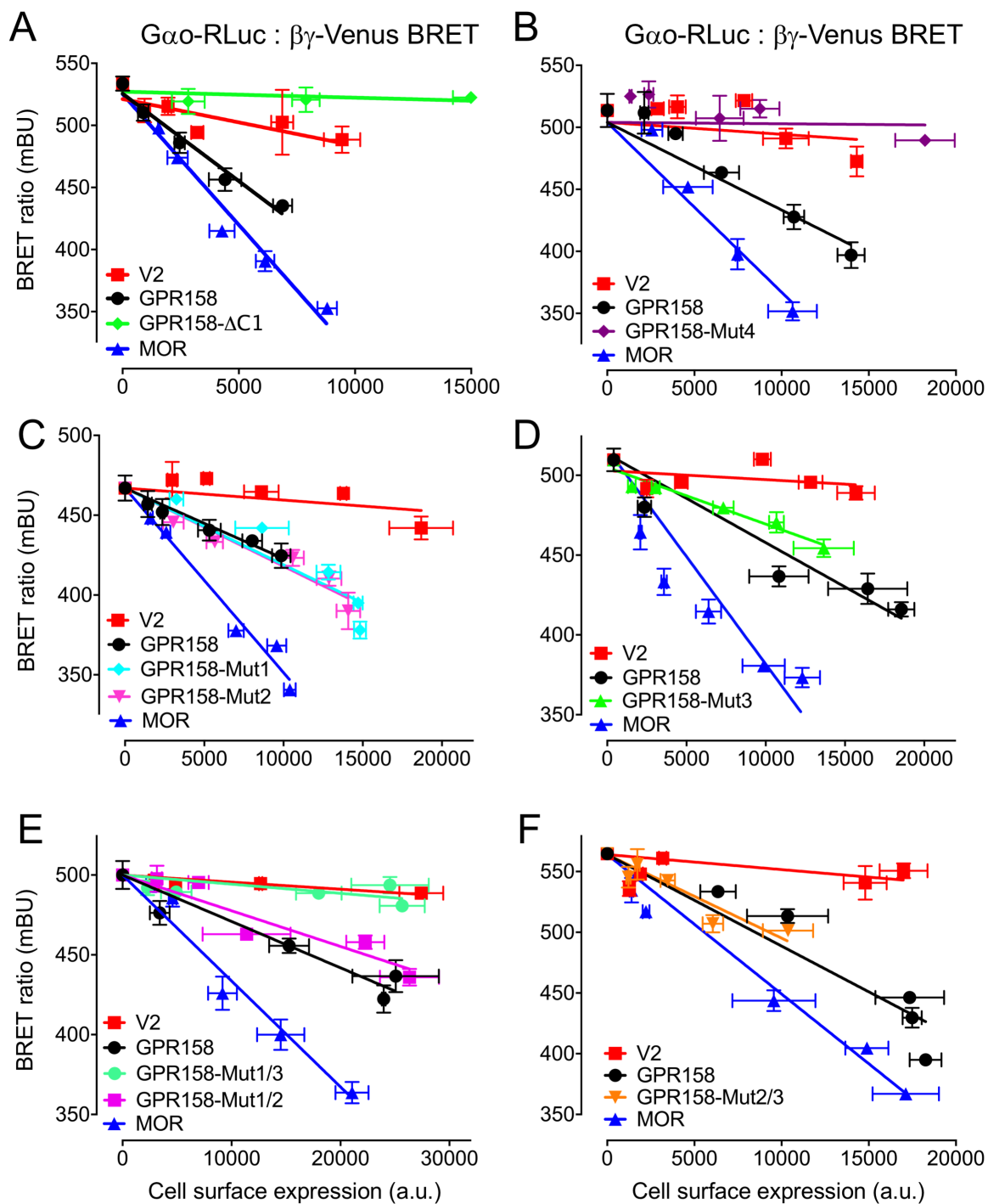


Figure 8